COMPUTATIONAL STUDIES OF NMR AND MAGNETO-OPTICAL ROTATION PARAMETERS IN WATER

TEEMU S. PENNANEN

Department of Physics
University of Oulu
Finland

Academic dissertation to be presented with the assent of the Faculty of Science, University of Oulu, for public discussion in the Auditorium YB210, on December 12$^{\text{th}}$ 2011, at 12 o'clock noon.

REPORT SERIES IN PHYSICAL SCIENCES Report No. 72
OULU 2011 • UNIVERSITY OF OULU

Opponent

Professor Dr. Ralf Ludwig, University of Rostock, Germany

Reviewers

Professor Dr. Ralf Ludwig, University of Rostock, Germany

Dr. Magdalena Pecul-Kudelska, University of Warsaw, Poland

Custos

Professor Juha Vaara, University of Oulu, Finland

ISBN 978-951-42-9730-4
ISBN (PDF) 978-951-42-9731-1
ISSN 1239-4327
Uniprint Oulu
Oulu 2011

Pennanen, Teemu S: **Computational Studies of NMR and Magneto-Optical Rotation Parameters in Water**
Department of Physics, University of Oulu, P.O.Box 3000, FIN-90014 University of Oulu, Finland, *Report Series in Physical Sciences No. 72 (2011)*

Abstract

In this thesis nuclear magnetic resonance (NMR) and magneto-optical rotation (MOR) parameters are investigated for water, paying special attention to the effect of solvation from gaseous to liquid phase. Nuclear magnetic shielding and quadrupole coupling tensors of NMR spectroscopy are studied for gaseous and liquid water. Liquid state is modelled by a 32-molecule Car-Parrinello molecular dynamics simulation, followed by property calculations for the central molecules in clusters cut out from the simulation trajectory. Gaseous state is similarly represented by a one-molecule simulation. Gas-to-liquid shifts for shielding constants obtained this way are in good agreement with experiments. To get insight into the local environment and its effect on the properties the clusters are divided into groups of distinct local features, namely the number of hydrogen bonds. The analysis shows in detail how the NMR tensors evolve as the environment changes gradually from the gas to liquid upon increasing the number of hydrogen bonds to the molecule of interest. The study sheds light on the usefulness of NMR experiments in investigating the local coordination of liquid water. To go a bit further, the above mentioned NMR parameters along with the spin-spin coupling constant are examined for water dimer in various geometries to have insight into solvation and hydrogen bonding phenomena from bottom to top. Characteristic changes in the properties are monitored as the geometry of the dimer is systematically varied from very close encounter of the monomers to distances and orientations where hydrogen bonding between monomers ceases to exist. No rapid changes during the hydrogen bond breaking are observed indicating that the hydrogen bonding is a continuous phenomenon rather than an on-off situation. However, for analysis purposes we provide an NMR-based hydrogen bond definition, expressed geometrically, based on the behaviour of the NMR properties as a function of dimer geometry. Our definition closely resembles widely used definitions and thus reinforces their validity.

Magneto-optical rotation parameters, the nuclear spin optical rotation (NSOR) and the Verdet constant, are computed for gaseous and liquid water, in the same manner as the NMR properties above. Recent pioneering experiments including NSOR for hydrogen nuclei in liquid water and liquid xenon have demonstrated that this technique has a potential to be a useful new probe of molecular structure. We reproduce computationally, applying a first-principles theory developed recently in the group, the experimental NSOR for hydrogen nuclei in liquid water, and predict hydrogen NSOR in gaseous water along with the oxygen NSOR in liquid and gaseous water. NSOR is an emerging experimental technique that needs interplay between theory and computation for validation, steering and insight.

Keywords: water, NMR, shielding constant, quadrupole coupling, spin-spin coupling, nuclear spin optical rotation, Faraday effect, quantum chemistry, molecular dynamics

Acknowledgements

The work presented in this thesis was carried out in the NMR Research Group at the Department of Physics of the University of Oulu during years 2004-2011. The former and present head of the Department of Physics, Prof. Jukka Jokisaari and Prof. Matti Weckström, are thanked for providing a pleasant working atmosphere and for providing the facilities at my disposal. Prof. Jukka Jokisaari and Prof. Juha Vaara and the entire NMR Research Group are thanked for creating an innovative and friendly working environment. Financial support from Väisälä Foundation, Finnish Cultural Foundation, Oulu University Scholarship Foundation, Research Foundation of Orion Corporation, The Finnish Foundation for Economic and Technical Sciences (KAUTE), Magnus Ehrnrooth Foundation, and Oulu University Pharmacy Foundation is acknowledged.

I would like to thank the reviewers of my thesis, Prof. Dr. Ralf Ludwig and Dr. Magdalena Pecul-Kudelska for their excellent work and valuable comments.

I thank the collaborators Dr. Atte J. Sillanpää, Prof. Kari Laasonen, Prof. Jukka Jokisaari, Dr. Mikko Hakala, and Suvi Ikäläinen for their contributions.

I am deeply grateful to my supervisors, Prof. Juha Vaara and Dr. Perttu Lantto, for their high quality mentoring and for their patience when the work has not been advanced as desired. Juha, I thank you for the interesting projects, excellent supervision and the pragmatic approach you have been emphasizing that helped me to focus on the tasks that can be done instead of dreaming about something bigger but impractical. I also thank you for the freedom I have been given that helped me to develop my own perspective about research. Perttu, I thank you for your high quality guidance and especially your invaluable know-how with computing and programs that are in daily use in our group. Many things would have been impossible to do on my own.

Matti, thank you for the many years we have been working together doing science. Your vast knowledge have been an immense help for me with innumerable computer-related problems. Thank you also for many interesting conversations about science, politics, economics, and other issues. A former member of the group Pekka T. is thanked for many interesting conversations about science. All former and present members of the NMR Research Group are thanked for the warm and cosy working atmosphere.

Many thanks go to my parents Arja and Pekka for their support in my studies and a positive attitude in life in general. You have encouraged me to chase my dreams and one such dream is about to happen... I am thankful to my siblings Harri and Titta for their

encouragement and mental support during this work.

Most of all, I thank my wonderful wife Elena who is an inspiration for me every single day. You are the most important person in my life and without you this work would have never been completed.

Oulu, November 2011, Teemu S. Pennanen

List of Original Papers

The present thesis consists of an introductory part and the following original papers, which are referred to in the text by their Roman numerals:

I Teemu S. Pennanen, Juha Vaara, Perttu Lantto, Atte J. Sillanpää, Kari Laasonen, and Jukka Jokisaari
Nuclear Magnetic Shielding and Quadrupole Coupling Tensors in Liquid Water: A Combined Molecular Dynamics Simulation and Quantum Chemical Study
Journal of the American Chemical Society **126**, 11093 (2004).

II Teemu S. Pennanen, Perttu Lantto, Atte J. Sillanpää, and Juha Vaara
Nuclear Magnetic Resonance Chemical Shifts and Quadrupole Couplings for Different Hydrogen-Bonding Cases Occurring in Liquid Water: A Computational Study
Journal of Physical Chemistry A **111**, 182 (2007).

III Teemu S. Pennanen, Perttu Lantto, Mikko Hakala, and Juha Vaara
Nuclear Magnetic Resonance Parameters in Water Dimer
Theoretical Chemistry Accounts **129**, 313 (2011).

IV Teemu S. Pennanen, Suvi Ikäläinen, Perttu Lantto, and Juha Vaara
Nuclear Spin Optical Rotation and Faraday Effect in Gaseous and Liquid Water,
manuscript submitted for publication.

The author of this thesis carried out most of the computational work, including quantum chemical calculations and analysis of the data, for all the Papers. Dr. Atte J. Sillanpää and professor Kari Laasonen carried out the Car-Parrinello simulations used in Paper I (this same simulation trajectory was also used in Papers II and IV). Dr. Perttu Lantto carried out a significant amount of the calibration and production calculations in Paper IV. Professor Juha Vaara carried out the treatment of the enhancement of the local electric field by the medium in the Paper IV. The author actively participated in the planning of the Papers II-IV. The first versions of the manuscripts were written by the author and

their were finished as teamwork. The programs used to analyze the data were mainly programmed by the author.

Abbreviations

B3LYP	Becke 3-parameter exchange functional plus Lee-Yang-Parr correlation functional
BHandHLYP	hybrid functional with half Becke exchange and half Hartree-Fock exchange, and LYP correlation part
BLYP	Becke exchange functional plus Lee-Yang-Parr correlation functional
CI	configuration interaction
CC	coupled cluster
CCSD	coupled cluster singles and doubles
CPMD	Car-Parrinello molecular dynamics
DSO	diamagnetic nuclear spin-electron orbit (operator, contribution)
FC	Fermi-contact (operator, contribution)
FCI	full configuration interaction
GGA	generalized gradient approximation
GIAO	gauge-including atomic orbital
HF	Hartree-Fock
LDA	local density approximation
LYP	Lee-Yang-Parr correlation functional
NSOR	nuclear spin optical rotation
NMR	nuclear magnetic resonance
MBPT	many body perturbation theory
MP	Møller-Plesset perturbation theory
MOR	magnetic optical rotation
PSO	paramagnetic spin-orbit (operator, contribution)
SD	spin-dipole (operator, contribution)

Contents

1 Introduction

1.1 Background

Water [1, 2] is perhaps the most important substance on Earth. It is an essential ingredient of all known forms of life. Being not only the most abundant substance in our bodies, it is also a cornerstone substance of any human society through everyday life used in drinking, cooking, washing, and cleaning, just name a few. Water is used in agriculture, power generation, food processing, etc. In chemistry, water is a universal solvent and many interesting chemical and biological processes take place in aqueous solutions. As ubiquitous and throughly investigated it is, there remain questions to be answered that are not only important for scientists but also for applications. As an example, a detailed molecular level structure of liquid water is constantly called into question [3–6]. The latest proposal [6] for a new structure started a heated debate lasting for many years [7–13]. These models are challenging the conventional, near tetrahedrally hydrogen-bonded model for liquid water.

Molecular level understanding of water is based on the interplay between experiments, "simple" theoretical models, quantum mechanical calculations, and simulations. New findings are constantly added to the vast amount of knowledge about water. It is important to develop new experimental techniques and refine the existing ones and, on the theoretical side, increase the number of details in the models and implement them in the programs for high-performance computations.

Nuclear magnetic resonance (NMR) spectroscopy [14, 15] is a widely used technique used to obtain physical, chemical and structural information about molecules in gaseous, liquid, solid and liquid crystal states of matter. Quantum chemistry [16] is a branch of theoretical chemistry that uses efficient numerical techniques and computational resources to solve chemically interesting problems using quantum mechanics. Simulations [17] (in the context of this thesis) are model systems that are used to produce the dynamics of the interacting many-particle (atoms, molecules) system, providing a direct route from the microscopic details of the model to macroscopic, measurable properties.

Modelling NMR parameters quantum chemically from first-principles is vital to complement the experiments, to obtain experimentally unavailable information and to make new predictions. Modelling solvation and taking into account the rovibrational effects in

the NMR parameters of water are important steps towards the ever-more increasing accuracy. Realistic comparison with results obtained by modern-day experimental equipment requires these effects to be accounted for. Here we use simulations to produce realistic liquid and gaseous state configurations at given temperature including the effects of classical rovibrational motion along with a neighbourhood the molecules experience in real liquid water. Subsequently, quantum chemical calculations are performed for a representative set of clusters cut out from simulations to obtain, after proper averaging, the NMR parameters of interest [18–20].

Magneto-optical detection of nuclear magnetization [21, 22] is a new experimental technique that has a potential to alleviate the difficulties associated with the conventional detection by NMR, the sensitivity and the resolution. It has been demonstrated to encode information on the chemical surroundings of the nucleus of interest [22, 23] resembling the chemical shift that makes the conventional NMR so useful. In the experiment the magnetic field associated with polarized nuclear spins rotates the plane of polarization of a laser beam traversing the material. This effect resembles the well-known effect of Faraday rotation [24, 25] and is called nuclear spin optical rotation (NSOR). In modelling of NSOR in water we use the same strategy as with the NMR parameters (taking clusters from simulations followed by quantum chemical calculations). For the calculations we use a first-principles theory recently developed in the group [22]. Computational and theoretical modelling of this emerging new technique is important in order to understand the detailed mechanisms of the phenomenon and to complement the experiments. It is exciting to participate in the studies involving a potentially important new field of physics and have a chance to contribute.

1.2 Outline of the thesis

In this thesis we study efficient methods to take care of the solvation and rovibrational effects in the modelling of water NMR and magneto-optical rotation (MOR) parameters. For NMR parameters of systems containing only light elements, these are thought to be the remaining factors that cause notable differences between experiment and computations. We use clusters cut out from water simulations and compute NMR properties for the center molecule in each cluster that is in a liquid water-like environment (Fig. 1.1). The results can be directly compared to the experimental measurements. In magneto-optical rotation our main target, NSOR, is a new pathway to explore nuclear magnetization through optical detection. Pioneering experiments with hydrogen nuclei in liquid water have only recently been published [21]. Our main objective is to computationally reproduce the results for hydrogen nuclei in liquid water and predict the corresponding effect for oxygen nuclei. Having established the applicability of the cluster technique in the case of water NMR we can confidently apply it to the NMR-related NSOR to include and assess the importance of environmental and rovibrational effects for this new, unexplored property.

In Paper I NMR shielding and quadrupole coupling tensors for oxygen and hydrogen nuclei in gaseous and liquid water are computed using Hartree-Fock [26–28] and density functional theory (DFT)/B3LYP [29–31] linear response methods using simulation

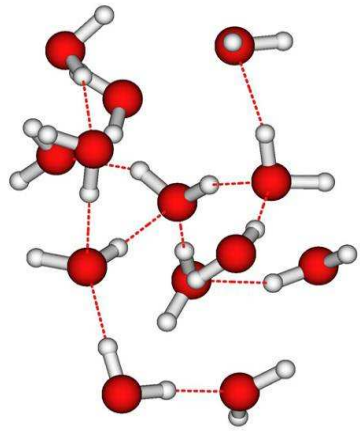

Figure 1.1. **A typical water cluster from Car-Parrinello molecular dynamics simulation. In this snapshot, center molecule (in the middle) has four hydrogen bonds.**

snapshots from Car-Parrinello [32] molecular dynamics trajectories. The NMR tensors are calculated and properly averaged for center molecules of 400 clusters representing the liquid. Similarly 400 instantaneous single molecule configurations from a gas-phase simulation represent the gaseous state. The difference between the liquid and gaseous state, the gas-to-liquid shifts, are found to be in good agreement with the experimental results. Full thermally averaged shielding and quadrupole coupling tensors, from which the usual NMR parameters are computed, are also reported for the gaseous and liquid state water.

Molecules in liquid water are in a constantly varying environment. Paper II extends the analysis of the NMR parameters beyond a simple liquid state average to shed light on the environmental details that may affect the NMR parameters. Clusters from Paper I are divided into groups that have similar local environments around their center molecules in terms of the number of hydrogen bonds. Full average NMR tensors and the usual NMR parameters derived from these tensors are calculated separately for each group. The analysis reveals in detail how the NMR tensors evolve as the environment gradually changes from the gas to liquid, upon increasing the number of hydrogen bonds (i.e. close neighbours) to the molecule of interest. The study shows how the local changes in the environment, including classical thermal averaging, affect the NMR parameters in liquid water. Results are also indicative of the NMR parameters in a confined environment, showing for example the effect of a broken or extra hydrogen bond. The data sheds light on the usefulness of NMR experiments in investigating the local coordination in liquid water.

Dimerization in water is the basic hydrogen bonding process. To shed light on the phenomenon and the impact of hydrogen bonding on NMR parameters of water, Paper III studies NMR parameter changes on dimerization of two water molecules. Shielding constants and anisotropies, quadrupole coupling constants and spin-spin coupling constants

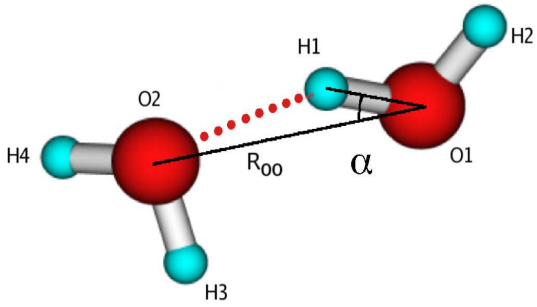

Figure 1.2. **Water dimer showing the hydrogen bond (red dots) and the two relevant geometric intermolecular parameters, the oxygen-oxygen distance $\mathrm{R_{oo}}$ and the hydrogen bond angle α.**

are monitored as the geometry of the dimer is varied. Dimer geometry is specified by two intermolecular parameters, the intermolecular oxygen-oxygen distance and the hydrogen bond angle, determining the mutual alignment of the two water molecules by dictating the distance and orientation between them. The two geometric parameters were systematically varied while monitoring the respective changes in NMR parameters which in turn are displayed as property surfaces for easy visualization. The analysis is extended beyond the total change by dividing it into the usually dominant, direct interaction effect and the indirect geometric effect. For analysis purposes we suggest a new pragmatic hydrogen bond definition based entirely on the NMR parameter trends on the property surfaces.

The magneto-optical rotation parameter NSOR for an isolated water molecule has recently been studied computationally [22] with the results in good agreement with experiment performed on liquid water [21]. Paper IV studies the NSOR and the Verdet constant computationally in gaseous and liquid water to assess the magnitude of the solvation and rovibrational effects on these properties. The same procedure that is succesfully applied in Papers I-II (water clusters from simulation fed into quantum chemistry program for the computation of properties) is used also here. The effect of solvation is found small for Verdet constant, but significant for the NSOR. However, medium enhances the local electric field in the liquid [33] (affecting both the Verdet constant and NSOR) which largely cancels the solvation effect for NSOR. Hydrogen NSOR is in good agreement with a recent pioneering experiment [21]. NSOR values for individual water molecules are found to have a broad distribution. We qualitatively link the extreme values to the corresponding hydrogen bonding situations.

In Chapter 2 of this thesis the computational methods including electronic structure calculation approaches and response theory for the computation of properties are covered. Chapter 3 presents the NMR and optical rotation parameters along with their computation. Chapter 4 is dedicated to water and its solvation modelling, introducing also briefly the simulations. Chapter 5 contains the summary of the Papers I-IV and Chapter 6 the conclusions.

2 Computational methods

2.1 Electronic structure calculation methods

Atoms and molecules are composed of nuclei and electrons. Nuclear structure in itself is a complicated field of research but a detailed structure is usually irrelevant for the molecular applications. The nuclei are merely regarded as point particles with well-defined properties such as charge, mass, spin, quadrupole moment, etc. For our water applications, amongst the nuclear properties only nuclear charge is used as an input parameter for the programs to compute the electronic structure. The electrons are treated quantum mechanically with a non-relativistic Schrödinger equation in a Born-Oppenheimer approximation [34], i.e., with a fixed nuclear framework.

Since nuclei are treated as point particles with classical properties, only electrons are treated quantum mechanically since no classical description is valid for them. The electrons are described by the Schrödinger equation

$$H\psi = \left(\frac{1}{2m_e} \sum_i p_i^2 - \frac{e^2}{4\pi\epsilon_0} \sum_i \sum_K \frac{Z_K}{r_{iK}} + \frac{e^2}{4\pi\epsilon_0} \sum_{i<j} \frac{1}{r_{ij}} \right) \psi = E\psi \qquad (2.1)$$

where H is the Hamiltonian operator, E is the energy, ψ is the wavefunction, Z is the nuclear charge, and r_{iK} is the distance between the electron i and nucleus K. Other symbols have their usual meanings. Solving the Schrödinger equation analytically is possible only for the most simple cases like the hydrogen atom because the electromagnetic Coulomb interaction between two or more quantum mechanical particles complicates the situation too much. Since exact solutions cannot be found, various approximations are employed to ease the problem. This leads to approximate solutions of the Schrödinger equation of varying quality. Much of practical quantum chemistry is choosing approximations that include the key features in the specific problems at a reasonable computational cost.

2.1.1 Basis set concept

One of the approximations that is inherent in practically all electronic structure methods is the introduction of a basis set [16]. The goal of solving the Schrödinger equation is to find the wave function and energy of the system. For molecules the many-body wavefunction is composed of one-electron functions called the molecular orbitals. The initially unknown molecular orbitals are expanded as linear combinations in a set of known functions, a basis set, also called atomic orbitals.

$$\phi_i = \sum_{\alpha}^{M} c_{\alpha i} \chi_\alpha \tag{2.2}$$

where ϕ represent the molecular orbitals, c the expansion coefficients, and χ the atomic orbitals. The use of a basis set enables a systematic, variational optimization of the coefficients in linear combinations to find the best possible molecular orbitals within that basis set. In order to describe the orbitals exactly the basis sets would need to be infinite. In practice finite basis sets are used.

There is a large number of different basis sets designed to achieve various goals in quantum chemistry. In this thesis we have mainly used well-known Dunning type basis set families [35–37] of increasing performance and have tested they applicability in our purposes thoroughly. For NSOR and Verdet constant calculations we have used a new type of basis set family developed in the group, the so-called completeness-optimized basis sets [22, 38].

2.1.2 Wavefunction-based methods

Wavefunction-based methods are conventional quantum mechanical methods that use the many-body wavefunction as a basic mathematical object in the theory. The goal of wavefunction methods is to find the wavefunction (and the energy) for the system in question since all measurable properties are in principle obtainable from the wavefunction. An approximation common to the main modern-day wavefunction methods is the Hartree-Fock approximation [26, 27]. Attempts to improve on the Hartree-Fock method are called post-Hartree-Fock methods and they can be made to converge systematically to the solution of the non-relativistic Schrödinger equation in the Born-Oppenheimer approximation.

2.1.2.1 Hartree-Fock method

Hartree-Fock (HF) method [26, 27] is a wavefunction approach that approximates the instantaneous electron-electron interaction as an average interaction and uses a single-determinantal description of the wavefunction. The Hartree-Fock method finds those spin-orbitals $\psi_1, \psi_2, ...$ that minimize the energy of the system described by one Slater determinant [39]

$$\Psi(\mathbf{x}_1, \mathbf{x}_2, \ldots, \mathbf{x}_N) = \frac{1}{\sqrt{N!}} \begin{vmatrix} \psi_1(\mathbf{x}_1) & \psi_2(\mathbf{x}_1) & \cdots & \psi_N(\mathbf{x}_1) \\ \psi_1(\mathbf{x}_2) & \psi_2(\mathbf{x}_2) & \cdots & \psi_N(\mathbf{x}_2) \\ \vdots & \vdots & & \vdots \\ \psi_1(\mathbf{x}_N) & \psi_2(\mathbf{x}_N) & \cdots & \psi_N(\mathbf{x}_N) \end{vmatrix} \tag{2.3}$$

For closed-shell molecules such as water a so-called Restricted Hartree-Fock theory is applied where all electrons are paired so that all spatial orbitals are doubly occupied with opposite spin electrons.

The introduction of the basis turns the Hartree-Fock equations into Roothaan equations [40, 41], which can be solved by standard matrix techniques. Finding molecular orbitals becomes finding the coeffiecients in the expansion of the molecular orbitals as linear combination of the basis functions. The Roothaan equations can be cast in a compact matrix equation as

$$\mathbf{FC} = \mathbf{SC}\varepsilon \tag{2.4}$$

where **F**,**C**, **S**, and ε are the Fock matrix, expansion coeffient matrix, overlap matrix, and a (diagonal) matrix of orbital energies, respectively. These non-linear equations are solved iteratively.

Hartree-Fock approximation is a reasonably good qualitative starting point for many important chemical applications such as calculating energies, equilibrium geometries, or ionization potentials [42]. As a matter of fact, the profound notion in chemistry of electrons residing in orbitals rests on the foundation that the Hartree-Fock approximation performs well in describing atomic or molecular systems with the wavefunction of only one Slater determinant expressed in terms of orbitals. Quantitative compatibility with experiments or more complex quantities require going beyond the Hartree-Fock approximation. Normally Hartree-Fock wavefunction is taken as a starting point for a more advanced post-Hartree-Fock calculation. The difference between the Hartree-Fock energy and the exact energy using the Schrödinger equation obtained with complete basis set is defined as the correlation energy. The term 'electron correlation' refers to everything left out in a Hartree-Fock approximation as compared to the exact results obtained using the Schrödinger equation. In practice, exact results for realistic systems are unattainable and only portions of electron correlation are recovered by post-Hartree-Fock methods. The choice of these electron correlation methods depends on the problem at hand.

2.1.2.2 Electron correlation methods

There are three main wavefunction based methods for including electron correlation: Configuration Interaction (CI), Many-Body Perturbation Theory (MBPT), and Coupled Cluster (CC) theory [16, 42]. All these take the Hartree-Fock wavefunction as a starting point and improve on that by including more than one Slater determinant. From these only the CC method [43–46] is used in this thesis for the electron correlation treatment.

In a restricted Hartree-Fock determinant the lowest energy molecular orbitals are doubly occupied and the rest of the orbitals, with their number dictated by the number of basis functions used, are unoccupied. By exciting one or more electrons from the occupied orbitals to those that are unoccupied in a Hartree-Fock determinant, we obtain singly, doubly, etc. excited determinants. It can be shown that the exact ground state wavefunction can be expressed as a linear combination of all possible Slater determinants from a complete set of basis functions. Different electron correlation methods truncate this linear combination by their own systematic way.

Configuration Interaction (CI) [42] is a method where singly, doubly, triply, etc. excited determinants, along with the Hartree-Fock determinant, are included in the wavefunction which is a linear combination of these determinants with the coeffiecients to be determined variationally by requiring the energy to be a minimum. CI method is variational (the energy is always an upper bound to the exact energy) but not size-extensive which means that the method does not scale properly with the number of particles. Thus the relative energies between systems are incorrect, which is a major drawback. If all the excited determinants are included in the wavefunction expansion we have Full Configuration Interaction (FCI), the best possible solution to the electronic problem for a given finite basis set. FCI is applicable only for small systems with small basis sets.

Many-Body Perturbation Theory [42] adds corrections to the wavefunction and energy to a given order. The choice of the unperturbed Hamiltonian to be a sum of Fock operators of HF theory is known as Møller-Plesset Perturbation Theory (MP) [47]. In effect, the MP includes all types of corrections (singles, doubles, etc.) to the unperturbed (Hartree-Fock) wavefunction to a given order [16]. A common, relatively inexpensive choice for including some of the electron correlation is the MP2 method where corrections up to second order are included. MP is size-extensive but not variational, which is not a serious problem since relative energies are more important than absolute energies.

The Coupled Cluster method includes all excitations of a given type to infinite order [16]. It uses a cluster operator A connecting the exact electronic wavefunction Ψ to the HF wavefunction Ψ_0 through

$$\Psi = e^A \Psi_0 \tag{2.5}$$

The exponential operator e^A is defined by $e^A = 1 + A + \frac{1}{2!}A^2 + \frac{1}{3!}A^3 + ...$ where A is the cluster operator $A = A_1 + A_2 + ... + A_N$. A_1 generates all determinants that are singly excited from the Hartree-Fock determinant, A_2 generates all determinants that are doubly excited, and so on:

$$A_1\Psi_0 = \sum_{a,p} t_a^p \Psi_a^p \quad , \quad A_2\Psi_0 = \sum_{a,b,p,q} t_{ab}^{pq} \Psi_{ab}^{pq} \quad , ... \tag{2.6}$$

The t_a^p, and t_{ab}^{pq} are single and double excitation amplitudes, and Ψ_a^p and Ψ_{ab}^{pq} are singly and doubly excited determinants. A widely used approximation is to truncate the cluster operator as A=A_1+A_2 which leads to the Coupled Cluster Singles and Doubles (CCSD) method. CCSD is the method used in this thesis as a reference to more approximate methods or when no experimental results are available. CC is size-extensive but not variational and it represents an excellent compromise between the accuracy and the computational cost for the molecules near equilibrium geometry.

2.1.3 Density functional theory

In density functional theory (DFT) [29] the electron density is the basic mathematical object that the theory is built on. The basis for the theory is the proof, by Hohenberg and Kohn [48], that the external potential is a unique functional of the electron density. Since the potential uniquely determines the ground state wavefunction, all other observables, including energy, are uniquely determined by electron density.

Electron density is a simple object as compared to the wavefunction since the density is a real function of the three-dimensional space, no matter how many electrons are involved. The energy of the system in question is connected with the electron density through a functional. Hence, the energy is available if the density is known. The problem is that the exact functional connecting the density and energy is not known. Developers of DFT are designing increasingly better functionals that approximate the elusive exact functional.

In DFT the electronic energy can be written as a functional of electron density ρ as [16]

$$E[\rho] = E_{ne}[\rho] + T[\rho] + E_{ee}[\rho] \tag{2.7}$$

where T, E_{ne}, E_{ee} are the kinetic energy, potential energy between nuclei and electrons, and potential energy between electrons. $E_{ee}[\rho]$ may be divided into Coulomb $J[\rho]$ and exchange parts $K[\rho]$ parts. The Kohn-Sham (KS) method [49] introduces one-electron functions (Kohn-Sham orbitals) with the idea that the kinetic energy consists of two parts, one that can be calculated exactly and another, small correction term. In the method, a non-interacting reference system is constructed, with the wavefunction a Slater determinant consisting of the Kohn-Sham orbitals, and having the same electron density as the interacting system in question. The reference system is used to calculate the major kinetic energy contribution (T_S). Then the energy can be expressed as

$$E[\rho] = T_S + E_{ne}[\rho] + J[\rho] + E_{xc}[\rho] \tag{2.8}$$

This expression defines the so-called exchange-correlation functional $E_{xc}[\rho]$ which consists of

$$E_{xc}[\rho] = (T[\rho] - T_S) + (E_{ee}[\rho] - J[\rho]) \tag{2.9}$$

The first part represents the remaining part of the kinetic energy that the non-interacting reference system cannot account for. The second term contains both the correlation energy ($J[\rho]$ represents the classical electron-electron Coulomb repulsion between the charge distributions corresponding to the KS orbitals) and exchange energy. The main problem in Kohn-Sham theory is designing functionals to represent the exchange-correlation energy. It is common to divide the exchange-correlation into exchange $E_x[\rho]$ and correlation $E_c[\rho]$ parts.

Various KS DFT methods differ only by they choice of the exchange-correlation functional. There are no systematic ways to improve DFT functionals in the same manner as there is a systematic way of improving the electron correlation treatment in wavefunction methods. There are, however, progressive steps in the development of functionals. Local Density Approximation (LDA) is a first step and it assumes that the density distribution can be locally treated as a uniform electron gas, accurately known from Quantum

Monte Carlo computations [50], which have been used to construct LDA correlation functional [51]. A second step is a non-uniform electron gas where exchange and correlaton energies depend also on the derivatives of the electron density. These are called generalized gradient approximations (GGA). The methods that use a portion of exact exchange and correlation from other sources are called the hybrid methods. We have mainly used BLYP [GGA functional with the Becke (B) exchange part and the Lee-Yang-Parr (LYP) correlation part] [52, 53], B3LYP (a hybrid functional with Becke 3-parameter exchange functional and LYP correlation part) [30, 31], and BHandHLYP (a hybrid functional with half Becke exchange and half Hartree-Fock exchange, with LYP correlation part) [54] functionals in this thesis. BLYP is used in Car-Parrinello simulations, B3LYP in NMR property calculations, and BHandHLYP in magnetic optical rotation calculations. These choices are based on experience on the applicability of the functionals to the various tasks, both from the literature and as acquired in the course of this work.

DFT is the most utilized computational method in this thesis due to its ability to include some electron correlation with small computational cost. Our large sample, extensive water clusters and moderate-sized basis sets would be a rather formidable task for any other correlation method. The Hartree-Fock method has also been used, mainly for testing and comparison purposes, but the performance is worse than that of DFT with appropriately chosen functional. Hartree-Fock calculations tend to underestimate the hydrogen bond strengths [55]. Weak dispersion interactions are poorly described by contemporary functionals [56, 57] but hydrogen bonding, being mainly electrostatic, is reasonably well described by DFT methods [16]. A comparison between DFT and different wavefunction methods for various hydrogen bonded dimers including water shows that DFT with a well chosen functional adequately describes dimers with linear hydrogen bonds [55]. A thorough benchmark investigation of equilibrium geometry and dissociation energy of the water dimer using different correlated wavefunction methods with high-quality basis sets serves as a performance test of the wavefunction methods in describing hydrogen bonding in water [58].

2.2 Computation of molecular properties

Determining the approximate wavefunction and the energy of a system are the basic steps in quantum chemistry. There are a number of molecular properties that can be computed by the use of a wavefunction. Most of these properties can be defined as the response of energy or some observable to a perturbation, where the pertubation may be any kind of operator absent in the Hamiltonian operator used to approximately solve the "unperturbed" Schrödinger equation [16]. External electric or magnetic fields are examples of such perturbations. The response theory is used in this work to calculate the NMR and magneto-optical rotation parameters.

2.2.1 Response theory

Response theory [59] describes the change of the expectation value of a property due to a perturbation. The perturbation may be an oscillating electric field describing monochromatic light of definite frequency, or some internal, static perturbation such as the nuclear magnetic moment. For time-dependent properties such as magnetic optical rotation parameters the response theory is the only practical means of making computational predictions. Static property calculations amount to response theory with zero perturbation frequency.

The expectation value of an operator P can be written in the presence of perturbations Q,R,... as [16]

$$\langle P\rangle(t) = \langle P\rangle(0)+\sum_k e^{-i\omega_k t}\langle\langle P;Q\rangle\rangle_{\omega_k}F_k+\frac{1}{2}\sum_{k,l}e^{-i(\omega_k+\omega_l)t}\langle\langle P;Q,R\rangle\rangle_{\omega_k,\omega_l}F_kF_l+... \tag{2.10}$$

where ω_k, ω_l, ... are the frequencies of the perturbations Q and R, respectively, and F_k,F_l, ... are the corresponding perturbation strengths, e.g. electric fields. The sum includes the expectation value followed by linear, quadratic, ... responses, which correspond to the second, third, ... order in time-dependent perturbation theory, respectively. The actual working equations for the calculation of response functions $\langle\langle P;Q\rangle\rangle$, $\langle\langle P;Q,R\rangle\rangle$, ... in electronic structure programs such as DALTON [60] are quite involved since they depend on the specific electronic structure method used. We provide references to the articles describing the implementation of the methods in the program package DALTON [60–63].

3 Nuclear magnetic resonance and magneto-optical rotation parameters

3.1 Basics of nuclear magnetic resonance

Some atomic nuclei possess internal angular momentum called spin, associated with a magnetic moment, which means that they can interact with a magnetic field. Nuclei with non-zero spin have more than one possible energy states when they are placed in a magnetic field. Transitions can be induced between these states by appropriate electromagnetic radiation, normally, in NMR, in the radio frequency range [14, 15]. Populations in different states at a temperature above zero Kelvin are not the same, leading to population differences and thus a net nuclear magnetization. The magnetization can be controlled by modern NMR spectrometers and its time dependence induces an oscillating electric field in a detector, producing a signal with a frequency that is proportional to the difference between the energy states of the nucleus. What is important in NMR is that the electronic environment of the nucleus affects the local magnetic field at the site of the nucleus and thus the energy differences in nuclear states. This so-called chemical shift carries information about the electronic structure around the nucleus. Different neighbourhood gives rise to a different chemical shift. It occurs due to the interaction between the nuclear spin and the magnetic field generated by the electrons around it. Other interactions that can have an effect on the NMR spectra include nuclear quadrupole coupling which results from the interaction of the nuclear electric quadrupole moment with the electric field gradient at the site of the nucleus generated by the electron cloud and other nuclei, and the spin-spin coupling which is due to the indirect mutual interaction of the two magnetic nuclei mediated by the electron cloud. These all fall into the category of the hyperfine interations, i.e., the interactions of the nucleus with its surroundings, other than the Coulomb interaction between the electrons and the nuclear charge.

3.1.1 NMR spin Hamiltonian

Experimental NMR spectrum is analyzed in terms of an effective NMR spin Hamiltonian which contains explicit expressions for interactions that may affect the spectrum. The interactions are represented by second rank tensors and the actual spectral parameters are specific combinations of the tensor elements as dictated by the nature of molecular tumbling (isotropic, partial orientation, orientational distribution in a powder sample) in the experimental conditions in question. Experiments provide the spectral parameters, not the entire tensors. In static water NMR there are two interactions that may affect the spectrum: shielding and spin-spin coupling, the latter among the nonequivalent nuclei.

The NMR spin Hamiltonian containing the aforementioned interactions for nucleus K in water can be written (in frequency units) as

$$H^K_{\mathrm{NMR}} = -\frac{1}{2\pi}\sum_K \gamma_K \mathbf{I}_K \cdot (\mathbf{1} - \boldsymbol{\sigma}_K) \cdot \mathbf{B}_0 + \sum_{K<L} \mathbf{I}_K \cdot (\mathbf{J}_{KL}) \cdot \mathbf{I}_L$$

Here γ_K, $\mathbf{I}_K$, and $\boldsymbol{\sigma}_K$ are the nuclear gyromagnetic ratio, nuclear spin, and shielding tensor for nucleus K, respectively. $\mathbf{B}_0$ is the external magnetic field, $\mathbf{1}$ is the 3x3 unit tensor, and $\mathbf{J}_{KL}$ is the spin-spin coupling tensor between two nuclei K and L. The water molecule may contain three NMR-active nuclei. ^{1}H is the normal hydrogen with spin $\frac{1}{2}$, ^{2}H (or ^{2}D) is the deuterium with spin 1, and ^{17}O is the isotope of oxygen with spin $\frac{5}{2}$. The most abundant oxygen isotope ^{16}O is not NMR-active (spin 0).

3.1.2 Shielding

When a molecule is placed in an external magnetic field $\mathbf{B}_0$, the magnetic field experienced by a certain nucleus $\mathbf{B}_K$ is not the same as the external field because the electronic structure around the nucleus responds to the external field, creating its own field that adds to the external field [64]. The extra field is described by the nuclear magnetic shielding tensor $\boldsymbol{\sigma}$ which depends on the electronic structure around the nucleus.

$$\mathbf{B}_K = (\mathbf{1} - \boldsymbol{\sigma}_K) \cdot \mathbf{B}_0 \tag{3.1}$$

In the isotropic phases such as in liquid or gaseous water the shielding tensor averages to the isotropic shielding constant, one-third of the trace of the shielding tensor. NMR experiments cannot provide the (absolute) shielding constants. They provide shielding constant differences, the chemical shifts. In computational work it is conventional to speak about shielding constants since calculations provide these directly. Shielding constants are expressed in parts per million (ppm) since they are usually small as compared to the nuclear Zeeman interaction (described by the unit tensor $\mathbf{1}$ in Eq. 3.1) which is the basis for the entire NMR experiment. For water the shielding constant of ^{17}O is around 300 ppm, and for hydrogen it is around 30 ppm, depending on the state. The chemical shift related to the difference between gaseous and liquid state water, the gas-to-liquid shift, is experimentally available for both the ^{17}O [65, 66] and ^{1}H [67, 68]. Gas-to-liquid shifts serve as

important experimental references to gauge the computational water NMR. Other spectral parameters available from the shielding tensor are the shielding anisotropy and the shielding asymmetry parameter that may be obtained experimentally in anisotropic phases such as liquid crystal solutions, or from relaxation experiments [69].

The nuclear magnetic shielding tensor is computed in two parts, a diamagnetic part, which is an expectation value of the ground state electronic wavefunction

$$\boldsymbol{\sigma}_K^d = \frac{e^2\hbar}{2m_e}\frac{\mu_0}{4\pi}\langle 0|\sum_i \frac{\mathbf{1}(\mathbf{r}_{iO}\cdot\mathbf{r}_{iK}) - \mathbf{r}_{iO}\mathbf{r}_{iK})}{r_{iK}^3}|0\rangle \tag{3.2}$$

and a paramagnetic part, which can be expressed as a linear response property

$$\boldsymbol{\sigma}_K^p = \frac{e^2\hbar}{2m_e^2}\frac{\mu_0}{4\pi}\langle\langle\sum_i \frac{\boldsymbol{\ell}_{iK}}{r_{iK}^3}; \sum_i \boldsymbol{\ell}_{iO}\rangle\rangle_{\omega=0} \tag{3.3}$$

Here K refers to the nucleus, i to the electrons, and O is the gauge origin. The non-relativistic shielding tensor is then a sum of the two contributions

$$\boldsymbol{\sigma}_K = \boldsymbol{\sigma}_K^d + \boldsymbol{\sigma}_K^p \tag{3.4}$$

Representation of the magnetic interaction operators corresponding to the external magnetic field is dependent on the choice of sc. gauge origin in the magnetic vector potential. For an exact wavefunction or Hartree-Fock wavefunction with complete basis set, the gauge origin would not cause any trouble, but practical, approximate calculations with incomplete basis sets give results that depend on the chosen origin [16]. This is a non-physical effect that should be corrected. The Gauge Including Atomic Orbital (GIAO) method [70, 71] eliminates the problem by making the basis functions dependent on the magnetic field by the inclusion of the complex phase factor. This removes the reference to an absolute gauge origin since matrix elements using GIAO orbitals contain only differences in vector potentials.

3.1.3 Quadrupole coupling

Nuclei with spin ≥ 1 (in water these may be ^{17}O with spin 5/2 or deuterium with spin 1) have a nuclear quadrupole moment which interacts with electric field gradients at the nuclear position. An electric field gradient appears if there is a non-spherical distribution of the charge density around the nucleus. The electric field gradient tensor is traceless so that it averages out in liquid and gaseous state water where the molecular tumbling is isotropic, but can be seen in anisotropic phases. Quadrupole coupling is a strong interaction in the realm of NMR and it is one of the possible relaxation pathways. This makes quadrupole coupling constants, for both the oxygen and the deuteron nuclei, measurable by NMR relaxation techniques in liquid state water [72]. The quadrupole coupling constant is the product of the largest principal component (eq) of the electric field gradient tensor and the nuclear electric quadrupole moment (eQ), a property of a nucleus.

The nuclear quadrupole coupling tensor is computed as an expectation value of the ground state plus a contribution from the nuclear charges at the positions $\boldsymbol{R}$ as

$$\mathcal{B}_K = \frac{e^2}{4\pi\epsilon_0}\frac{Q_K}{2I_K(2I_K-1)h}\left[\sum_{L\neq K} Z_L \frac{3\boldsymbol{R}_{KL}\boldsymbol{R}_{KL}-\mathbf{1}R_{KL}^2}{R_{KL}^5} - \langle 0|\sum_i \frac{3\boldsymbol{r}_{iK}\boldsymbol{r}_{iK}-\mathbf{1}r_{iK}^2}{r_{iK}^5}|0\rangle\right]. \quad (3.5)$$

3.1.4 Spin-spin coupling

Nuclear spins are little magnets with associated magnetic fields. Hence, they can interact also with themselves, either directly through dipole-dipole coupling or indirectly with the help of the electronic system through indirect spin-spin coupling [64]. The direct dipole-dipole coupling is not of interest in this thesis. It averages out in isotropic phases such as liquid or gaseous state water. Indirect spin-spin coupling is mediated through the electronic system by a modification of the wavefunction around a nucleus K by hyperfine interactions, then transmitted elsewhere in the electronic system by mutual electron-electron interactions, and finally felt by another nucleus L, again through hyperfine interaction. This splits the energy states of a nucleus and consequently its resonance signal into two or more lines. Spin-spin coupling is expressed in Hz.

The spin-spin coupling constant is a sum of four contributions

$$J_{KL} = J_{KL}^{\mathrm{DSO}} + J_{KL}^{\mathrm{PSO}} + J_{KL}^{\mathrm{SD}} + J_{KL}^{\mathrm{FC}} \quad (3.6)$$

Diamagnetic spin-orbit contribution is a ground state expectation value

$$J_{KL,\epsilon\tau}^{\mathrm{DSO}} = \frac{1}{2\pi}\hbar\gamma_K\gamma_L\frac{e^2}{2m_e}(\frac{\mu_0}{4\pi})^2\langle 0|h_{KL,\epsilon\tau}^{\mathrm{DSO}}|0\rangle \quad (3.7)$$

of the diamagnetic nuclear spin-electron orbit operator

$$h_{KL,\epsilon\tau}^{\mathrm{DSO}} = \sum_i \frac{(\boldsymbol{r}_{iK}\cdot\boldsymbol{r}_{iL})\delta_{\epsilon\tau} - r_{iL,\epsilon}r_{iK,\tau}}{r_{iK}^3 r_{iL}^3} \quad (3.8)$$

Paramagnetic nuclear spin-electron orbit J_{KL}^{PSO}, spin-dipole J_{KL}^{SD}, and Fermi contact J_{KL}^{FC} contributions can be expressed using response theory notation as

$$J_{KL,\epsilon\tau}^{\mathrm{PSO}} = \frac{1}{2\pi}\hbar\gamma_K\gamma_L\frac{e^2}{m_e^2}(\frac{\mu_0}{4\pi})^2\langle\langle h_{K,\epsilon}^{\mathrm{PSO}}; h_{L,\tau}^{\mathrm{PSO}}\rangle\rangle_0 \quad (3.9)$$

with the paramagnetic nuclear spin electron orbit operator

$$h_{K,\epsilon}^{\mathrm{PSO}} = \sum_i \frac{\boldsymbol{\ell}_{iK,\epsilon}}{r_{iK}^3}, \quad (3.10)$$

$$J_{KL,\epsilon\tau}^{\mathrm{SD}} = \frac{1}{2\pi}\hbar\gamma_K\gamma_L\frac{1}{4}\frac{e^2\hbar^2}{m_e^2}(\frac{\mu_0}{4\pi})^2 g_e^2 \sum_{\nu=x,y,z}\langle\langle h_{K,\epsilon\nu}^{\mathrm{SD}}; h_{L,\tau\nu}^{\mathrm{SD}}\rangle\rangle_0 \quad (3.11)$$

with the spin-dipole operator

$$h^{\mathrm{SD}}_{K,\epsilon\tau} = \sum_i \frac{3r_{iK,\epsilon}r_{iK,\tau} - \delta_{\epsilon\tau}r^2_{iK}}{r^5_{iK}} s_{i,\epsilon}, \tag{3.12}$$

and the diagonal Fermi contact contribution

$$J^{\mathrm{FC}}_{KL,\epsilon\epsilon} = \frac{1}{2\pi}\hbar\gamma_K\gamma_L \frac{16\pi^2}{9}\frac{e^2\hbar^2}{m_e^2}(\frac{\mu_0}{4\pi})^2 g_e^2 \langle\langle h^{\mathrm{FC}}_{K,\epsilon}; h^{\mathrm{FC}}_{L,\epsilon}\rangle\rangle_0 \tag{3.13}$$

with the Fermi contact operator

$$h^{\mathrm{FC}}_{K,\epsilon} = \sum_i \delta(\boldsymbol{r}_{iK}) s_{i,\epsilon} \tag{3.14}$$

In the formulas 3.8, 3.10, 3.12, and 3.14 the prefactors of the operators are included in the response expressions 3.7, 3.9, 3.11, and 3.13, respectively, γ is the nuclear gyromagnetic ratio, $\delta(\boldsymbol{r}_{iK})$ is the Dirac delta function at the nuclear position, $\boldsymbol{\ell}_{iK}$ is the angular momentum of electron i with respect to nucleus K, g_e is the free-electron g-factor, and s_i is the electron spin. The full $\boldsymbol{J}$ tensor also contains SD/FC cross term.

3.2 Optical rotation parameters

Optical rotation is the turning of the plane of linearly polarized light about the direction of motion as it traverses a material. When magnetic field in the direction of the light beam causes the optical rotation, the phenomenon is called either Faraday rotation (external field) or nuclear spin optical rotation (field from spin-polarized nuclei). Both are governed by closely related physics [22].

Linearly polarized light can be decomposed into left and right circularly polarized components [73]. The rotation of the plane of the linearly polarized light takes place when the indices of refraction for the two components differ; one of the components is then lagging behind. The angle of rotation is

$$\theta = \frac{\omega l}{2c}(n_- - n_+) \tag{3.15}$$

where ω is the frequency of the light, l is the distance travelled in the medium, c is the speed of light in vacuum, and n_- and n_+ correspond to the indices of refraction for the left and right circular polarization, respectively. In general, the index of refraction is a tensor and is related to the polarizability (when $n \approx 1$) as

$$n_{\varepsilon\tau} = \delta_{\varepsilon\tau} + \frac{\mathcal{N}}{2\epsilon_0}\langle\alpha_{\varepsilon\tau}\rangle \tag{3.16}$$

where $\delta_{\varepsilon\tau}$ is the Kronecker delta (unit tensor), $\mathcal{N}$ is the number density of molecules, and $\alpha_{\varepsilon\tau}$ is the polarizability tensor. The indices of refraction for the left and right circular polarizations correspond to particular tensor components $n_- = n_{YX}$ and $n_+ = n_{XY}$, for a light beam travelling in the Z direction. Normally, the polarizability is a symmetric

tensor and the two tensor elements n_{YX}, n_{XY} are equal. However, in the presence of a magnetic interaction the wave function becomes complex resulting in a complex, antisymmetric contribution (denoted here as $\alpha'_{\varepsilon\tau}$) to the polarizability tensor. This makes the left and right circularly polarized components travel with different speeds. The antisymmetric polarizability in the presence of the magnetic field (from either $\boldsymbol{B}_0$ or $\boldsymbol{I}_K$) can be written as

$$\alpha'_{\varepsilon\tau}(\boldsymbol{B}_0) = \sum_\nu \alpha'^{(B_0)}_{\varepsilon\tau,\nu} B_{0,\nu} \quad ; \quad \alpha'_{\varepsilon\tau}(\boldsymbol{I}_K) = \sum_\nu \alpha'^{(I_K)}_{\varepsilon\tau,\nu} I_{K,\nu} \tag{3.17}$$

In terms of response functions expressed in a molecule-fixed cartesian coordinate system, the antisymmetric polarizability due to external field ($\alpha'^{(B_0)}_{\varepsilon\tau,\nu}$) or due to hyperfine field ($\alpha'^{(I_K)}_{\varepsilon\tau,\nu}$) can be written as

$$\alpha'^{(B_0)}_{\varepsilon\tau,\nu} = -\langle\langle \mu_\epsilon; \mu_\tau, h^{\rm OZ}_\nu \rangle\rangle_{\omega,0} \quad ; \quad \alpha'^{(I_K)}_{\varepsilon\tau,\nu} = -\langle\langle \mu_\epsilon; \mu_\tau, h^{\rm PSO}_\nu \rangle\rangle_{\omega,0} \tag{3.18}$$

where $\boldsymbol{\mu}$ ($= -e\boldsymbol{r}$) is electric dipole moment, and $h^{\rm OZ}_\nu (= \frac{e}{2m_e}\sum_i \ell_{iO,\nu})$ and $h^{\rm PSO}_\nu$ are the orbital Zeeman and the orbital hyperfine interactions, respectively. The measurable rotation angle can be shown to be [74, 75]

$$\Phi = \frac{1}{2}\omega l \mathcal{N}\mu_0 c\, {\rm Im}\langle\alpha'_{XY}\rangle \tag{3.19}$$

For the external magnetic field $\boldsymbol{B}_0 = B_0\hat{\boldsymbol{Z}}$ or the average spin polarization $\langle \boldsymbol{I}_K\rangle = \langle I_{K,Z}\rangle\hat{\boldsymbol{Z}}$ in the Z direction in a medium where the molecules are isotropically tumbling:

$$\langle\alpha'_{XY}\rangle = B_0 \frac{1}{6}\sum_{\epsilon\tau\nu} \varepsilon_{\epsilon\tau\nu}\alpha'^{(B_0)}_{\varepsilon\tau,\nu} \quad ; \quad \langle\alpha'_{XY}\rangle = \langle I_{K,Z}\rangle \frac{1}{6}\sum_{\epsilon\tau\nu} \varepsilon_{\epsilon\tau\nu}\alpha'^{(I_K)}_{\varepsilon\tau,\nu} \tag{3.20}$$

where $\varepsilon_{\epsilon\tau\nu}$ is the Levi-Civita tensor.

For Faraday optical rotation the relation between the angle of rotation $\Phi_{\rm F}$ and the magnetic field B_0 is expressed in terms of a proportionality parameter, the Verdet constant V, as $\Phi_{\rm F}$=VB_0l. Using the arguments and the notation sketched above, the Verdet constant can be written as [22]

$$V = -\frac{1}{2}\,\omega\mathcal{N}\mu_0 c\,\frac{e^3}{2m_e}\,\frac{1}{6}\sum_{\epsilon\tau\nu}\varepsilon_{\epsilon\tau\nu}{\rm Im}\langle\langle r_\epsilon; r_\tau, \ell_{O,\nu}\rangle\rangle_{\omega,0} \tag{3.21}$$

The Verdet constant has been experimentally determined for gaseous [76] and liquid water [76–78]. For the nuclear spin optical rotation (NSOR) corresponding to the magnetic field from spin-polarized nuclei we obtain (for a molar concentration $[\,] = \frac{\mathcal{N}}{N_{\rm A}}$) [22]

$$\begin{aligned}\frac{\Phi_{\rm NSOR}}{[\,]\,l} &= -\frac{1}{2}\,\omega N_{\rm A} c\langle I_{K,Z}\rangle\,\frac{e^3\hbar}{m_e}\,\frac{\mu_0^2}{4\pi}\,\gamma_K \\ &\quad \times\frac{1}{6}\sum_{\epsilon\tau\nu}\varepsilon_{\epsilon\tau\nu}{\rm Im}\langle\langle r_\epsilon; r_\tau, \frac{\ell_{K,\nu}}{r_K^3}\rangle\rangle_{\omega,0}\end{aligned} \tag{3.22}$$

NSOR has only recently been, for the first time, experimentally determined [21] for hydrogen nuclei in liquid water and for liquid xenon. Only few theoretical papers have appeared on the subject [22, 79]. A first-principles theory on the subject has been published very recently [22]. In the same paper, NSOR was predicted to exhibit a similar effect as the chemical shift in NMR, the "optical chemical shift" [22] between similar nuclei in different chemical surroundings such as different functional groups or different molecules. An experimental demonstration of this effect appeared simultaneously [23].

4 Water

4.1 Modelling solvation effects for water NMR parameters

NMR parameters in gaseous water may be appropriately modelled by single molecule calculations with a suitable rovibrational treatment. Modelling NMR parameters in liquid water calls for a proper treatment of the solvent neighbourhood including the rovibrational effects [80, 81]. Static solvation effects may be modelled, for example, by including neighbouring molecules in an actual calculation alongside with the molecule of interest or by using continuum solvation models [82, 83]. In a continuum solvation model, the molecular system placed in a cavity of dielectric continuum representing the solvent polarizes the continuum by inducing multipole moments which, in turn, act as a source of secondary electric field that acts on the molecule in question. However, continuum solvation models alone have been shown not to describe solvation effects on the NMR shielding constants faithfully [20, 84]. A reasonably good description is obtained by the use of the first explicit solvation shell plus a continuum model around this cluster [85]. Dynamic solvation effects from a continuously changing molecular environment and the classical rovibrational effects are included by using clusters from simulations with the interest on the properties of the center molecule [18–20]. It has been observed that static cluster solvation performs worse than dynamic solvation for the NMR gas-to-liquid shifts in water [86]. When comparing continuum and cluster models it was observed that dynamic cluster model gave the best results [84]. In this thesis, we used a combined dynamic cluster plus continuum model that explicitly treated clusters of 10-19 molecules from simulation and the remaining long-range effect by a continuum model. Other approaches for the computations of solvation effects on the NMR parameters of interest include the computations "on the fly" during the simulation using the same periodic framework as for the electronic structure calculation used to generate the simulation trajectory [87], and a related approach for the calculation of NMR shielding constants in periodic systems [88].

The NMR gas-to-liquid shift is a sensitive measure of the intermolecular interactions. It is well-known for protons [67, 68] and oxygen [65, 66] in water, and serves as an excellent test for computational methods [20, 84, 86, 87, 89, 90]. Calculated and experimental gas-to-liquid shifts with different methods are displayed for oxygen in Table 4.1 and for hydrogen in Table 4.2.

Table 4.1. Calculated and Experimental ^{17}O Nuclear Shielding Constant and Gas-to-Liquid Shift in Water.[a]

Method	$\sigma(g)$	$\sigma(l)$	$\delta = \sigma(l) - \sigma(g)$
HF[b]	311.0±0.9	286.7±0.6	−24.3±1.4
B3LYP[b]	309.7±0.9	268.5±0.6	−41.2±1.5
Exp.	323.6±0.6 [c]	287.5±0.6	−36.1[d]
HF[e]			−20.3±9.6
HF[f]	336.6	320.2	−16.4
LDA[g]			−36.6±0.5
PW91[h]			−37.6±2.1
PBE0[i]			−34.8
BLYP[j]			−30
RASSCF[k]	324.0±1.5		

[a] In ppm. [b] Present work, with 400 samples taken from a CPMD trajectory. [c] Reference [91] based on the experimental determination of the spin-rotation constant of ^{17}O in carbon monoxide ^{12}C^{17}O [92]. [d] Reference [66]. [e] Reference [86] using 30 decamers from MD simulation. [f] Reference [85]. Static cluster model where the central molecule was explicitly solvated by four surrounding molecules and a dielectric continuum. [g] Reference [90]. Including 9 snapshots containing the whole MD simulation cell of 32 molecules. The reference is a single molecule at the equilibrium geometry. [h] Reference [89]. Extrapolated cluster calculations (40 clusters) sampled from a MD trajectory generated using an empirical potential energy function. [i] Reference [84]. Using a mixed explicit/continuum solvation model. Clusters of eleven molecules were taken from a MD simulation with the molecules kept at the fixed, optimized geometry. [j] Reference [87]. [k] Reference [93]. Contains a quantum mechanically calculated rovibrational correction of −12.04 ppm (for the ^{1}H$_2$^{17}O isotopomer).

Table 4.2. Calculated and Experimental ^{1}H Nuclear Shielding Constant and Gas-to-Liquid Shift in Water.[a]

Method	$\sigma(g)$	$\sigma(l)$	$\delta = \sigma(l) - \sigma(g)$
HF[b]	29.52±0.06	24.38±0.09	−5.14±0.14
B3LYP[b]	30.07±0.05	24.80±0.08	−5.27±0.13
Exp.[c]	30.052±0.015	25.79	−4.26
HF[d]			−2.28±1.61
HF[e]	30.91	26.94	−3.97
LDA[f]			−5.83±0.10
PW91[g]			−3.22±0.20
BLYP[h]			−4.1
RASSCF[i]	30.2±0.1		

[a] In ppm. [b] Present work. [c] References [67, 68]. [d] See footnote e in Table 4.1. [e] See footnote f in Table 4.1. [f] See footnote g in Table 4.1. [g] See footnote h in Table 4.1. [h] See footnote j in Table 4.1. [i] See footnote k in Table 4.1. Contains a quantum mechanically calculated rovibrational correction of −0.549 ppm (for the ^{1}H$_2$^{17}O isotopomer).

4.2 Simulations and Car-Parrinello method

Explicit solvation requires the knowledge of the positions of all the nuclei in the cluster, i.e., the inner and relative geometries of all the molecules. In the case of water, these are not known in detail. In fact, a detailed microscopic structure of liquid water has been a matter of debate from time to time. The last "big" debate, starting from X-ray absorption measurements [6] which were interpreted to mean that liquid water is mainly composed of chains and rings rather than a tetrahedral network of water molecules, raised a lot of dialogue [7–13]. There are ways to make educated guesses on how molecules are located relative to one another. Partial information is available from experiments but at present there is no experiment that would reveal the detailed structure. Apart from just guessing the positions, one can simulate [17] the behaviour of the water system. In molecular dynamics simulation the forces between molecules are calculated from first principles or from classical force fields and molecules are moving according to the Newton's laws of motion. We use first principles Car-Parrinello molecular dynamics (CPMD) [32] simulations.

CPMD approach is a combination of molecular dynamics and density functional theory to perform simulations. In this method the total-energy functional is optimized by the simulated annealing method [94] using the Kohn-Sham orbital coefficients as variational parameters. CPMD allows the bond forming and breaking in the course of the simulation, which extends its usefulness as compared to the classical force-field type simulations. The forces between the molecules are computed by a quantum mechanical density functional theory method and there is no need for a pre-parametrized force-field as is the case in classical simulations. The quality of the calculated forces depends on the functional used. In CPMD simulations, where a large number of water molecules (typically 32-64 [95–97] but sometimes over 200 [98] as compared with a typical quantum chemical calculation using 1-10 mols) are treated by DFT, the functional has to be chosen so that the computations are not too heavy. A classic choice for a CPMD water functional is BLYP [52, 53] as is the case also in this thesis. The simulations were carried out by Dr. A. J. Sillanpää and Prof. K. Laasonen [99].

4.3 Water structure and hydrogen bonding

There are no experimental techniques at the moment that would reveal the exact positions of water molecules in liquid water, i.e., the microscopic structure of liquid water. X-ray or neutron diffraction experiments provide radial pair-correlation functions but these are isotropic: they do not reveal the orientations of water molecules with respect to one another [1]. NMR spectroscopy chemical shifts provide averages over all molecules and over a time span large compared to the time scale relevant for molecular motions, thus blurring a detailed image. Computations with highly accurate wavefunction-based electronic structure methods with appropriate basis sets for large water ensembles are not possible due to the large computational burden. Theoretically, water simulations give detailed information about positions of molecules around each other, but they still have many shortcomings, related to the use of classical force-fields, small system sizes, quan-

tum motion for light nuclei, etc. Thus, the positional data provided by simulations should be understood to be somewhat incomplete [100]. Studying small water complexes, clusters, gives information about structure and bonding, and acts as a bridge between the gaseous and condensed phases of water [101, 102].

A traditional view of liquid water is that molecules have on average about four hydrogen bonds (HBs) that are located in a (nearly) tetrahedral manner around each molecule [103], see Fig. 1.1. These HBs constantly break and reform and there may be "under" or "over" bonded species [Paper II] at any given instant. Molecules may also have non-hydrogen bonded neighbours that are in unfavourable positions or orientations in order to form proper HBs. Simulations may be analyzed according to local environment, for example the number and type of hydrogen bonds [Paper II]. There are conventionally two types of hydrogen bond criteria to judge whether two molecules have a mutual HB, geometric or energetic criteria [104]. Energetic criteria are usually based on the pair-interaction energy between two molecules [105]. Geometric criteria usually use distance and angle cut-offs in order to identify the pair of hydrogen bonded molecules [106, 107]. However, energy and NMR parameters are continuous functions of dimer geometry [Paper III] suggesting that hydrogen bonding is a continuous (instead of an on/off) phenomenon. Conventional hydrogen bond criteria discard this aspect but remain useful for analysis purposes. A personal view of the author is that no detailed criterion for hydrogen bonding exists and it could be beneficial for the field if the phenomenon of hydrogen bonding would be approached in a more continuous manner.

5 Summary of the Papers

5.1 Papers I-II: Solvation effect on water NMR parameters

Molecules may be computationally modelled at their equilibrium geometry in vacuo. For NMR parameters the omission of the solvation and rovibrational effects cause notable differences between experiment and computations [80]. Finding efficient methods for taking these effects into account in water is the major objective in this thesis. Attaining experimentally unavailable information, such as the full NMR shielding tensors of liquid state water, is one of the advantages of the computational research. Computational averaging of anisotropic molecular properties, such as individual tensor components, is rarely done since it requires the use of the Eckart frame, an appropriate coordinate system which rotates with the molecule while providing a maximum separation of the rotational and vibrational degrees of freedom, allowing a component-wise addition of the tensor elements [108], [Paper I].

Paper I reports the full NMR shielding and quadrupole coupling tensors averaged in the Eckart coordinate frame for the gaseous and liquid state water using Hartree-Fock and DFT/B3LYP methods, for snapshots sampled from Car-Parrinello molecular dynamics trajectories at 300 K. A recent computational study [109] suggests the usage of DFT/B3LYP with (practically) the same basis set as ours for proton and ^{17}O shielding constants in small water clusters. The NMR tensors were calculated for 400 center molecules in clusters representing the liquid and 400 instantaneous single-molecule configurations from a gas-phase simulation. Liquid clusters of size 10-19 molecules with an average cluster 14-15 molecules guarantee that the first and much of the second solvation shell were included. The usual NMR parameters are also reported. The difference between the gaseous and liquid-state shielding constants, the gas-to-liquid shift, available directly from experiments is in good agreement for ^{17}O (Table 4.1: within 15% using DFT/B3LYP) and for hydrogen (Table 4.2) within 20%.

We have recognized and used different methods of averaging for the NMR parameters that are anisotropic (for example for the shielding anisotropy and the quadrupole coupling constant). One involves averaging the full tensors in the Eckart frame, diagonalizing them and using the principal components to calculate the anisotropic parameters. This method is recognized to correspond to static NMR experiments in an anisotropic medium. The second method uses diagonalized instantaneous tensors to compute the

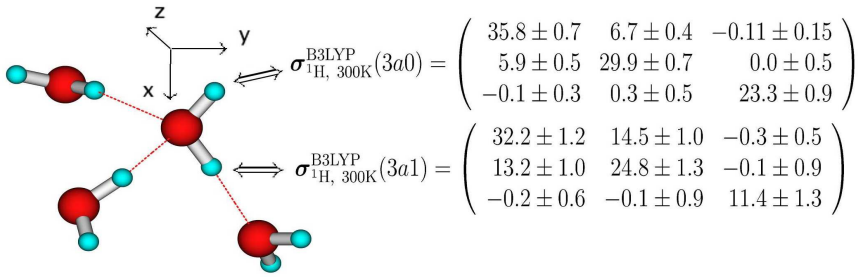

Figure 5.1. **A schematic representation of a portion of water cluster with the center molecule having three hydrogen bonds showing the NMR shielding tensors for the hydrogen nucleus of the center molecule, either having a hydrogen bond (3a1) or not (3a0). The tensors are averages of the (3a1) and (3a0) cases expressed in Eckart frame indicated in the figure. Notable differences are observed between the two cases. The calculations include the whole clusters and not just the small part displayed here.**

anisotropic parameters (e.g. instantaneous eigenvalues) and the averaging is performed afterwards. This method corresponds better to relaxation experiments since it uses the instantaneous principal components presented in the instantaneous principal axis frame of the molecules. Since the two methods yield different results it must be concluded that, formally speaking, the operations of averaging and diagonalization do not commute, i.e., the result depend on the order of the operations. This is not a problem since the two methods correspond to different experimental set-ups.

In liquid water the molecular environment is constantly changing, hydrogen bonds forming and breaking. NMR parameters for individual molecules change accordingly. To shed light on the nature of these changes, Paper II extended the analysis of the NMR tensors and parameters beyond the average liquid state values. Water clusters from Paper I were divided into groups that have similar local environments in terms of the hydrogen bond number, using a simple distance-based criterion. Full NMR tensors and the usual NMR parameters were determined for each group. We used a simple one-parameter definition to identify the hydrogen bonds. This results in an average hydrogen bond number slightly larger than four. The hydrogen bond number for single molecules ranges from two to six, four being by far the most abundant species. Five HBs is the second most abundant, followed by three HBs, 6 or 2 HBs being rare in our sample of 400 clusters. The location of individual HBs within the species 3 and 5 allow further subcategories, see for example Figs. 5.1 and 5.2.

Systematic changes in the average NMR parameters as a function of hydrogen bond number are observed. An almost linear dependence of the NMR parameters as a function of the HB number is observed from gaseous (no HBs) to four HBs where a plateau is reached, see Figure 6 in Paper II. Distributions of single-molecule values are displayed revealing the range and "concentration" of individual NMR parameters for each hydrogen bonding case, see Fig. 5.3. In general, the distributions are wide and overlapping. Gaseous

and liquid state distributions differ appreciably in shape and the location of their center of gravity. A short explanation for the differing shapes is that the shape of the gaseous distribution is a reminiscent of the position distribution of the classical harmonic oscillator while in the liquid the presence of the neighbours does not allow harmonic oscillations of the covalent r_{OH} bonds. A stochastic nature of the neighbour interactions makes the liquid state distribution to be Gaussian in shape. A more thorough discussion is given in Paper II.

The analysis reveals how the full NMR tensors evolve as the surroundings of the center molecule of each cluster gradually change from gaseous type into full liquid-like environment and shows in detail how changes in the local environment of a water molecule affect its NMR parameters, see Fig. 5.2. Results are indicative of the NMR parameters in con-

$$\boldsymbol{\sigma}^{\mathrm{B3LYP}}_{^{17}\mathrm{O}}(g) = \begin{pmatrix} 341.7 \pm 1.0 & 0.0 \pm 0.5 & 0.0 \pm 0.0 \\ 0.0 \pm 0.4 & 300.0 \pm 0.9 & 0.0 \pm 0.0 \\ 0.0 \pm 0.0 & 0.0 \pm 0.0 & 287.5 \pm 0.9 \end{pmatrix}$$

$$\boldsymbol{\sigma}^{\mathrm{B3LYP}}_{^{17}\mathrm{O}}(2) = \begin{pmatrix} 306.1 & -7.7 & -0.4 \\ -4.6 & 278.0 & 14.3 \\ -0.5 & 8.8 & 267.3 \end{pmatrix}$$

$$\boldsymbol{\sigma}^{\mathrm{B3LYP}}_{^{17}\mathrm{O}}(3a) = \begin{pmatrix} 295 \pm 5 & -5 \pm 5 & -4 \pm 4 \\ -3 \pm 4 & 273 \pm 5 & 2 \pm 3 \\ -1 \pm 2 & 2 \pm 2 & 258 \pm 5 \end{pmatrix}$$

$$\boldsymbol{\sigma}^{\mathrm{B3LYP}}_{^{17}\mathrm{O}}(3d) = \begin{pmatrix} 308 \pm 3 & -3 \pm 3 & -2.4 \pm 1.1 \\ 3 \pm 3 & 271 \pm 4 & 0 \pm 2 \\ 0.1 \pm 0.6 & -0.8 \pm 1.5 & 256 \pm 4 \end{pmatrix}$$

$$\boldsymbol{\sigma}^{\mathrm{B3LYP}}_{^{17}\mathrm{O}}(4) = \begin{pmatrix} 289.7 \pm 1.0 & 0.1 \pm 0.6 & -0.1 \pm 0.5 \\ 0.1 \pm 0.6 & 261.1 \pm 0.9 & -0.3 \pm 0.4 \\ -0.2 \pm 0.3 & 0.0 \pm 0.4 & 253.1 \pm 0.8 \end{pmatrix}$$

$$\boldsymbol{\sigma}^{\mathrm{B3LYP}}_{^{17}\mathrm{O}}(5a) = \begin{pmatrix} 293 \pm 4 & 2 \pm 2 & 2.8 \pm 1.2 \\ 2.9 \pm 1.7 & 261 \pm 4 & -1 \pm 2 \\ 2.0 \pm 0.7 & -0.5 \pm 1.3 & 252 \pm 3 \end{pmatrix}$$

$$\boldsymbol{\sigma}^{\mathrm{B3LYP}}_{^{17}\mathrm{O}}(5d) = \begin{pmatrix} 288 \pm 3 & 1.7 \pm 1.4 & 0.5 \pm 0.8 \\ 2.0 \pm 1.2 & 262 \pm 2 & 1.0 \pm 0.8 \\ 0.5 \pm 0.4 & 0.3 \pm 0.8 & 253 \pm 2 \end{pmatrix}$$

$$\boldsymbol{\sigma}^{\mathrm{B3LYP}}_{^{17}\mathrm{O}}(6) = \begin{pmatrix} 280 \pm 6 & 3 \pm 6 & 1 \pm 3 \\ 2 \pm 6 & 246 \pm 3 & 5 \pm 4 \\ 1.6 \pm 1.1 & 4 \pm 2 & 247 \pm 4 \end{pmatrix}$$

$$\boldsymbol{\sigma}^{\mathrm{B3LYP}}_{^{17}\mathrm{O}}(l) = \begin{pmatrix} 290.7 \pm 0.8 & 0.3 \pm 0.5 & 0.0 \pm 0.4 \\ 0.7 \pm 0.5 & 261.7 \pm 0.8 & 0.0 \pm 0.4 \\ 0.1 \pm 0.2 & 0.1 \pm 0.4 & 253.2 \pm 0.7 \end{pmatrix}$$

Figure 5.2. Average ^{17}O nuclear magnetic shielding tensors (in ppm) for water in the liquid and gaseous states, and for the various hydrogen-bonding species in the liquid at 300 K. The number in parentheses gives the number of hydrogen bonds (HBs) for the center molecule, see Fig. 5.3 for details. The molecule is in the xy plane, with the C_2 axis in the y direction, see Fig. 5.1. The error limits for the two-fold hydrogen-bonded species have been omitted due to the small size of the statistical sample.

fined environments where there might be missing or extra hydrogen bonds. A broken HB induces major changes in the NMR parameters which can be seen by comparing hydrogens with or without the HB, see Fig. 5.1. The NMR parameters of hydrogens without HB resemble the gaseous state parameters, as expected, while the hydrogens with the HB are close to the average liquid values. NMR parameters of the different hydrogen bonding species in water are not experimentally available and it is anticipated that their detection would be difficult since the distributions have significant overlap.

Papers I-II testify about the usefulness of the method of using clusters from simulation to model the solvation effects in liquid water NMR. The use of density functional

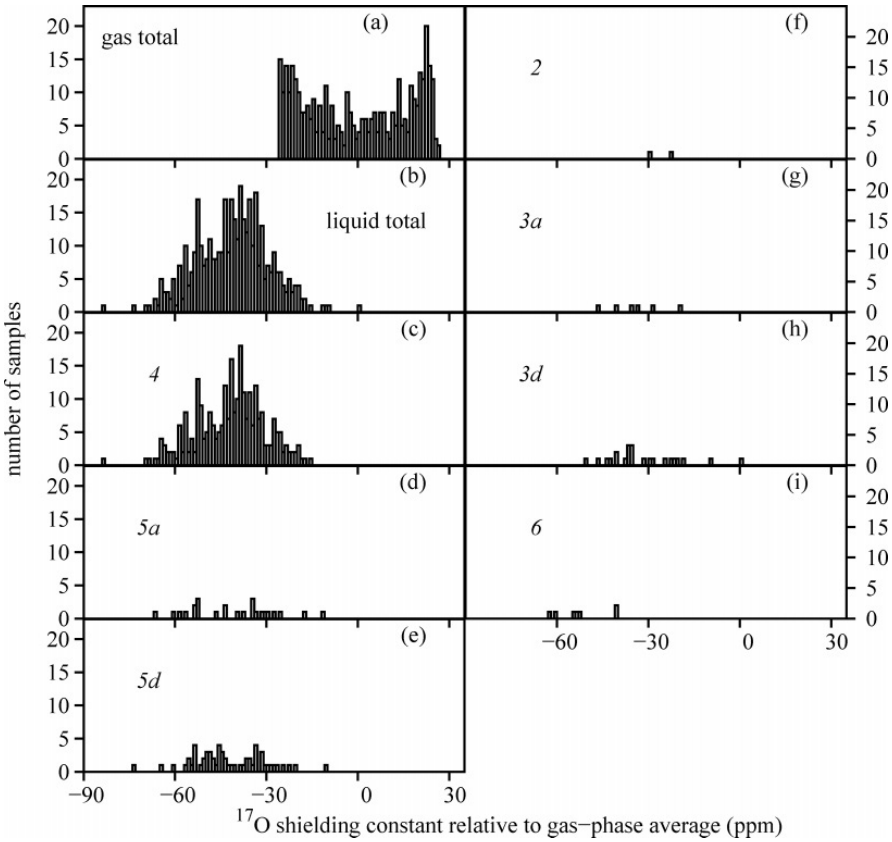

Figure 5.3. Distributions of the isotropic ^{17}O shielding constant for liquid and gaseous water at 300 K, broken down to the various hydrogen-bonding species. Panels: (a) total distribution for gas, (b) total distribution for liquid, (c) liquid molecules with 4 hydrogen bonds (HBs), (d) 5 HBs, with an extra hydrogen-bond acceptor molecule (*5a*), (e) 5 HBs, with an extra hydrogen-bond donor molecule (*5d*), (f) 2 HBs, (g) 3 HBs, acceptor molecule missing (*3a*), (h) 3 HBs, donor molecule missing (*3d*), and (i) 6 HBs.

theory is mandatory since the clusters are relatively large and the Hartree-Fock level is not good enough for these properties. Our results are in good agreement with available experiments. The method can be used, after calibrations and case-specific modifications, to model solvation effects outside the field of NMR, as in Paper IV.

5.2 Paper III: NMR parameters in water dimer

Hydrogen bonding in water is an archetype of this interesting phenomenon. To study hydrogen bonding process from the perspective of NMR, Paper III studies NMR parameter changes upon dimerization of two water molecules. The study gives a detailed account of the changes that are expected in NMR parameters when two water molecules are in close encounter. It also gives insight into hydrogen bonding effects in liquid state water from "bottom to top".

Shielding constants and anisotropies, quadrupole coupling constants and spin-spin coupling constants were monitored as the geometry of the dimer was varied systematically. Dimer geometry was specified by two intermolecular parameters, the intermolecular oxygen-oxygen distance and the hydrogen bond angle, see Fig. 1.2. The other geometrical parameters of the dimer were allowed to relax while keeping the aforementioned two parameters fixed. Varying the two geometric parameters appropriately creates a grid of possible dimer geometries that are indicative of the mutual orientation of two water molecules in any real situation in which they might interact with each other such as in gaseous or liquid water. The NMR parameters were computed with DFT/B3LYP for each grid point and displayed as property surfaces for easy visualization of the characteristic changes of different NMR parameters, see Fig. 5.4. Spin-spin couplings [110] and shielding constants [111–113] in water dimer have been studied computationally before. A recent study [113] compared different functionals with CC calculations in water dimer and formaldehyde in complex with two water molecules, suggesting the superiority of the KT3 functional over B3LYP in shielding constants. Our computations reveal that the performance of the B3LYP is no inferior to KT3 functional when all NMR parameters are taken into account.

All NMR parameters are smoothly behaving as the dimer geometry is varied. This indicates that there is no abrupt change associated with the breaking of a hydrogen bond which suggests that hydrogen bonding is a continuous instead of an on-off type phenomenon. For practical purposes we suggest a geometric hydrogen bond definition based entirely on the NMR parameter behaviour on the property surfaces. Our definition, $R_{\mathrm{OO}} \leq 3.5$ Å and $\alpha \leq 45°$, closely resembles the traditional hydrogen bond definitions [104, 106, 107] and thus reinforces their validity.

The analysis was extended by dividing the total change into direct interaction effect and the indirect geometric effect. The division is enabled by a transformation of an isolated monomer in monomer geometry, to a monomer in dimer geometry with a neighbour, i.e., an interacting dimer, with the help of two operations: the change of monomer geometry into the dimer geometry and the introduction of a neighbour. The direct interaction effect is found to dominate the indirect geometric effect in all cases, but the geometric effect should be included as well, see Table. 5.1. In the process, we observed a fundamental

ambiguity in this type of partitioning, arising from the different order in which the two above-mentioned operations can be performed. The order affects the individual partitions (but not their sum) as can be clearly seen for σ_{O1} in Table. 5.1. The non-commutativity of the two operations resembles the situation in Paper I where different methods could be used in calculating the average anisotropic properties. It is a reminder that an unphysical operation (e.g. a geometry change without a cause) may lead to an ambiguous result.

The ambiguousness is noticed to be intimately related to a pairwise additive approximation (PAA). This approximation assumes that contributions, for example to NMR parameters, from neighbouring atoms or molecules can be separately evaluated and accumulated, and that the investigated molecule need not to be relaxed geometrically after adding each neighbour, since the geometric effect can be added afterwards if necessary [114]. The latter condition fails if the geometry change and the addition of the neighbour are

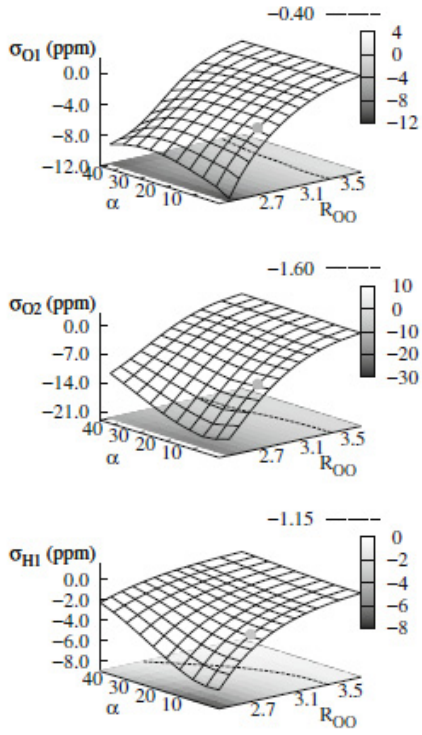

Figure 5.4. B3LYP/aug-cc-pCVTZ NMR shielding surfaces of the water dimer for the donor oxygen O1, acceptor oxygen O2, and hydrogen-bonded hydrogen H1 as a function of the intermolecular oxygen-oxygen distance R_{OO} and hydrogen-bond angle α. The marked point indicates the equilibrium geometry and the black projected curve is an equipotential contour corresponding to the value at the point R_{OO}=3.5 Å and α=0°.

Table 5.1. **Comparison of the direct intermolecular interaction effect and the indirect geometric effect for shielding constants in the water dimer. The diagram shows the different partitions into direct and geometric effects obtained using two auxiliary intermediate states. State(1) is a monomer in a geometry it assumes in an interacting dimer. State(2) is a dimer where both water molecules are in their monomer geometries. (See Paper III for details).**

			state(1)		
		Δgeom(1)		Δdirect(1)	
	mon		Δ(dim-mon)		dim
		Δdirect(2)		Δgeom(2)	
			state(2)		
			323.6		
		-1.9		-2.3	
σ_{O1}	325.5		-4.2		321.3
		-2.9		-1.3	
(ppm)			322.6		
			325.1		
		-0.4		-8.6	
σ_{O2}	325.5		-9.0		316.5
		-8.6		-0.4	
(ppm)			316.9		
			30.79		
		-0.29		-2.84	
σ_{H1}	31.08		-3.13		27.96
		-2.77		-0.36	
(ppm)			28.32		

not independent operations. The connection between the order of the two operations and PAA may be used as an easy test whether a certain property is pairwise additive without resorting to the full pairwise additive process. In cases where PAA holds the property surfaces may provide an easy way to compute condensed phase properties without expensive cluster calculations by combining them with position data from simulations [81]. For example, for quadrupole couplings in liquid water, PAA is observed to be a good approximation [114].

5.3 Paper IV: Solvation effect on NSOR and Verdet constant in water

Nuclear spin optical rotation is an emerging new field of physics that has a potential to become a useful tool for studying molecules and materials. NSOR has recently been measured for liquid water [21] but studied computationally only for an isolated water

molecule [22]. Modelling solvation and rovibrational effects are important steps towards a more realistic description for NSOR in liquid water. Computational studies predicted new important effects like the optical chemical shift [22], verified also experimentally [23]. To understand the detailed mechanisms of this new field, it is important to develop theory [22] and perform computations under realistic experimental conditions as well as predict and explain new phenomena.

In paper IV, magneto-optical rotation parameters, the NSOR and the Verdet constant, were computed for gaseous and liquid water using DFT/BHandHLYP [30] with completeness-optimized (co) Gaussian basis sets [38], to assess the importance of solvation effects on these properties. We used the same procedure as was succesfully applied in Papers I-II: instantaneous water clusters from simulation fed into quantum chemistry program for the computation of properties.

The direct solvation effect for NSOR is found to be -14% and -29% for ^{1}H and ^{17}O nuclei, respectively. However, the medium influences also the local optical field at the site of the molecule [33] and not only the response properties of a single molecule. Hence, the properties should be corrected for the local optical field (affecting both the Verdet constant and NSOR), which largely cancels the solvation effect for NSOR. Hydrogen NSOR is in good agreement with a recent pioneering experiment [21]. Besides simulation averages for liquid and gas, single molecule calculations, with CCSD used for referencing purposes, were performed in order to assess the rovibrational and geometry change effects, see Fig. 5.5. The NSOR values for individual water molecules are found to have a broad distribution and we qualitatively link the extreme values to the corresponding local hydrogen bonding situations.

The same methodology as used in calculating solvation effects for NMR parameters has proven its transferability, working well also in the realm of optical rotation parameters. The competing effects of direct solvation and the enhancement of the optical local field explain why isolated single molecule calculations [22] compared so favourably with experimentally measured hydrogen NSOR in liquid water [21].

We found useful, based on the observed behaviour of the Verdet constant, to introduce a new concept, the Verdet constant per molecule (V_1), which is potentially a useful concept in the future. It is based on the observation, related to the extensive nature of this property, that contributions to the Verdet constant from any molecule in a cluster are about the same size. The Verdet constants reported in this study refer to this V_1. The direct solvation effect for V_1 is found to be small. However, the monomer geometry change has an appreciable effect which can be seen from single molecule calculations in different geometries.

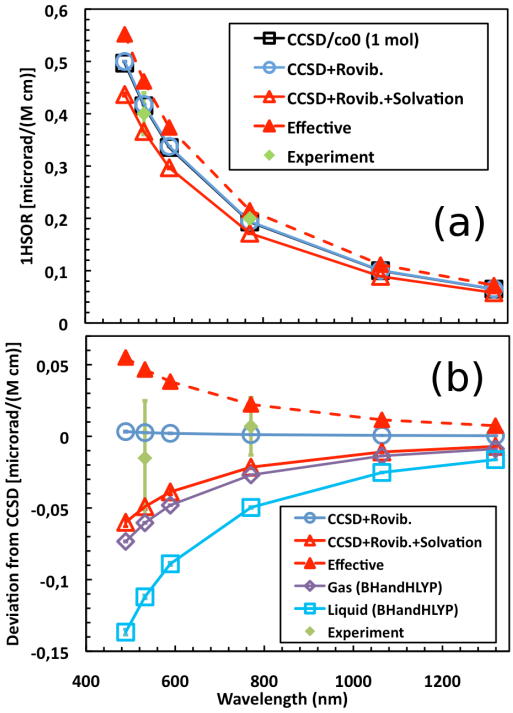

Figure 5.5. **(a) ^{1}H spin optical rotation angle for water showing the best equilibrium-geometry calculation for a static, isolated molecule [CCSD/co0 (1 mol)], corrected cumulatively for rovibrational, solvation, and local electric field (Effective) influences. The experimental results [21] are displayed with the error margins, whereas the statistical error of the calculations is small in the scale of the figure. (b) The deviation of the data of panel (a) from the CCSD/co0 (1 mol) result. The directly simulated gas- and liquid-state values are also shown.**

6 Conclusions

Water is one of the most important substances on Earth. Understanding its behaviour at the molecular level requires the interplay between the experiment, theory, and computations. Nuclear magnetic resonance is a widely used tool to obtain physical, chemical and structural information on the molecules and materials. A quantitatively accurate comparison of theoretically obtained results with experiments requires systems to be modelled realistically. This involves including the solvent and rovibrational effects in the realm of NMR for molecules containing only light elements [80]. Optical rotation caused by aligned nuclear spins is a new field that may open new windows to study molecules and materials [21]. In this thesis we use efficient methods to take these effects into account for NMR and optical rotation parameters in water.

The research covered in this thesis is essentially two-fold. First, a rather thorough investigation of water static NMR parameters, including gaseous and liquid water [Papers I-II] followed by water dimer NMR study [Paper III] essentially applicable to all situations where two water molecules can closely interact under normal conditions. Secondly, a computational investigation was performed on the parameters in liquid and gaseous water of a new field of physics, optical detection of nuclear magnetization [Paper IV]. This nuclear spin optical rotation may prove as an important experimental method to overcome the known sensitivity and spatial resolution problems in usual NMR and magnetic resonance imaging. Papers I-III cover the usual NMR parameters in water. On the other hand, water can be studied from the perspective of NSOR detecting the same nuclear magnetization in a different way, as in Paper IV.

The main results include the solvation effects in liquid water for NMR shielding and quadrupole coupling tensors and the usual NMR parameters, the shielding and quadrupole coupling constants. Special attention is paid to the averaging of the anisotropic properties which is rarely done. Two different ways to average anisotropic properties are observed and identified to correspond to different methods of experimental detection. Constantly changing local environment in liquid water is investigated by dividing water clusters in groups having different number of hydrogen bonds attached to the center molecule. The analysis of the corresponding changes in the NMR parameters reveals in detail, for example, the effects of missing or extra hydrogen bonds. The study of water dimer in different geometries on the perspective of NMR parameters gives a detailed account on the effects of hydrogen bonding in the dimerization, or in case where two water molecules are in

close encounter. All NMR parameters are behaving smoothly as the dimer geometry is varied. A division of the total effect into direct interaction effect and the indirect, geometric effect revealed an interesting connection to the pairwise additivity. A by-product is a test to be used whether a certain parameter is pairwise additive or not. Pairwise additivity may reduce computational cost of condensed phase properties appreciably. Direct solvation effect and the enhancement of the local optical field on NSOR and Verdet constant in gaseous and liquid water have been computed and compared with experiments in Paper IV. The hydrogen NSOR is in good agreement with a recent pioneering experiment in liquid water. Based on the observed behaviour of Verdet constant in water clusters, we have introduced a new concept, Verdet constant per molecule, which may turn out to be useful in future studies.

The application of the current methodology of clusters from simulations and subsequent property calculations has been proven useful in these studies including gaseous and liquid water for NMR and optical rotation parameters. This technique can be used to take care of the solvent and rovibrational effects in condensed phases with a reasonable computational cost. The use of density functional theory is mandatory if quantitative agreement with experiments is desired because of its excellent compromise between cost and accuracy. Getting experimentally unattainable information is one of the motivation behind computational methods. For example, we have presented full NMR tensors along with the usual measurable NMR parameters. Besides the main objectives, we have identified, incorporated and discussed many interesting, experimentally unavailable, aspects of the theoretical methodology. These by-products may prove useful in the future.

Conventional NMR is a well-known subject with established theory that would require a vast amount of knowledge and expertise to make useful contributions. NSOR, instead, is a new field with only a handful of articles published on the subject. Any contribution has a potential to become significant or even ground-breaking since the first steps in a new field are guided by the few that are involved. I am grateful for the chance to be involved and I hope I could be creative and open minded enough to be able to contribute.

Bibliography

[1] D. Eisenberg and W. Kauzmann, *The Structure and Properties of Water* (Oxford University Press, London, 1969).

[2] F. Franks, ed., *Water: A Comprehensive Treatise, Vols 1-7* (Plenum Press, New York, 1972-1982).

[3] M. Vedamuthu, S. Singh, and G. W. Robinson, J. Phys. Chem. **98**, 2222 (1994).

[4] A. Khan, R. Khan, M. F. Khan, and F. Khanam, Chem. Phys. Lett. **266**, 473 (1997).

[5] F. Weinhold, J. Chem. Phys. **109**, 373 (1998).

[6] P. Wernet, D. Nordlund, U. Bergmann, M. Cavalleri, M. Odelius, H. Ogasawara, L. Å. Näslund, T. K. Hirsch, L. Ojamäe, P. Glatzel, et al., Science **304**, 995 (2004).

[7] J. D. Smith, C. D. Cappa, K. R. Wilson, B. M. Messer, R. C. Cohen, and R. J. Saykally, Science **306**, 851 (2004).

[8] L. Å. Näslund, J. Lüning, Y. Ufuktepe, H. Ogasawara, P. Wernet, U. Bergmann, L. G. M. Pettersson, and A. Nilsson, J. Phys. Chem. B **109**, 13835 (2005).

[9] A. Nilsson, P. Wernet, D. Nordlund, U. Bergmann, M. Cavalleri, M. Odelius, H. Ogasawara, L. Å. Näslund, T. K. Hirsch, L. Ojamäe, et al., Science **308**, 793a (2005).

[10] J. D. Smith, C. D. Cappa, B. M. Messer, R. C. Cohen, and R. J. Saykally, Science **308**, 793b (2005).

[11] J. D. Smith, C. D. Cappa, K. R. Wilson, R. C. Cohen, P. L. Geissler, and R. J. Saykally, Proc. Natl. Acad. Sci. U.S.A. **102**, 14171 (2005).

[12] T. Head-Gordon and M. E. Johnson, Proc. Natl. Acad. Sci. U.S.A. **103**, 7973 (2006).

[13] J. D. Smith, C. D. Cappa, B. M. Messer, W. S. Drisdell, R. C. Cohen, and R. J. Saykally, J. Phys. Chem. B **110**, 20038 (2006).

[14] A. Abragam, *The Principles of Nuclear Magnetic Resonance* (Oxford University Press, Oxford, 1961).

[15] C. P. Slichter, *Principles of Magnetic Resonance* (Springer-Verlag, Berlin, 2nd ed., 1990).

[16] F. Jensen, *Introduction to Computational Chemistry* (John Wiley & Sons Ltd, Chichester, 2nd ed., 2007).

[17] M. P. Allen and D. J. Tildesley, *Computer Simulation of Liquids* (Clarendon Press, Oxford, 1987).

[18] K. Hermansson, S. Knuts, and J. Lindgren, J. Chem. Phys. **95**, 7486 (1991).

[19] R. Eggenberger, S. Gerber, H. Huber, D. Searles, and M. Welker, J. Chem. Phys. **97**, 5898 (1992).

[20] D. B. Searles and H. Huber, in *Encyclopedia of Nuclear Magnetic Resonance, Volume 9: Advances in NMR,* edited by D. M. Grant and R. K. Harris (John Wiley & Sons, Ltd: Chichester, 2002).

[21] I. M. Savukov, S. K. Lee, and M. V. Romalis, Nature **442**, 1021 (2006).

[22] S. Ikäläinen, M. V. Romalis, P. Lantto, and J. Vaara, Phys. Rev. Lett. **105**, 153001 (2010).

[23] D. Pagliero, W. Dong, D. Sakellariou, and C. A. Meriles, J. Chem. Phys. **133**, 154505 (2010).

[24] M. Faraday, Philos. Mag. **28**, 294 (1846).

[25] M. Faraday, Philos. Trans. R. Soc. London **136**, 1 (1846).

[26] D. R. Hartree, Proc. Cambr. Phil. Soc. **24**, 328 (1928).

[27] V. A. Fock, Z. Phys. **15**, 126 (1930).

[28] J. C. Slater, Phys. Rev. **35**, 210 (1930).

[29] R. G. Parr and W. Yang, *Density-Functional Theory of Atoms and Molecules* (Oxford University Press, Oxford, 1989).

[30] A. D. Becke, J. Chem. Phys. **98**, 5648 (1993).

[31] P. J. Stephens, F. J. Devlin, C. F. Chabalowski, and M. J. Frisch, J. Phys. Chem. **98**, 11623 (1994).

[32] R. Car and M. Parrinello, Phys. Rev. Lett. **55**, 2471 (1985).

[33] R. Wortmann and D. M. Bishop, J. Chem. Phys. **108**, 1001 (1998).

[34] M. Born and R. Oppenheimer, Ann. Phys. **389**, 457 (1927).

[35] Th. H. Dunning, Jr., J. Chem. Phys. **90**, 1007 (1989).

[36] R. A. Kendall, Th. H. Dunning, Jr., and R. J. Harrison, J. Chem. Phys. **96**, 6796 (1992).

[37] D. E. Woon and Th. H. Dunning, Jr., J. Chem. Phys. **103**, 4572 (1995).

[38] P. Manninen and J. Vaara, J. Comput. Chem. **27**, 434 (2006).

[39] J. C. Slater, Phys. Rev. **34**, 1293 (1929).

[40] C. C. J. Roothaan, Rev. Mod. Phys. **23**, 69 (1951).

[41] G. G. Hall, Proc. R. Soc. Lond. A **205**, 541 (1951).

[42] A. Szabo and N. S. Ostlund, *Modern Quantum Chemistry: Introduction to Advanced Electronic Structure Theory* (Dover, New York, 1996).

[43] J. Čižek, J. Chem. Phys. **45**, 4256 (1966).

[44] J. Čižek, Adv. Chem. Phys. **14**, 35 (1969).

[45] J. Čižek and J. Paldus, Int. J. Quantum. Chem. **5**, 359 (1971).

[46] O. Sinanoğlu, J. Chem. Phys. **36**, 706 (1962).

[47] C. Møller and M. S. Plesset, Phys. Rev. **46**, 618 (1934).

[48] P. Hohenberg and W. Kohn, Phys. Rev. **136**, B864 (1964).

[49] W. Kohn and L. J. Sham, Phys. Rev. **140**, A1133 (1965).

[50] D. M. Ceperley and B. J. Alder, Phys. Rev. Lett. **45**, 566 (1980).

[51] J. P. Perdew, E. R. McMullen, and A. Zunger, Phys. Rev. A **23**, 2785 (1981).

[52] A. D. Becke, Phys. Rev. A **38**, 3098 (1988).

[53] C. Lee, W. Yang, and R. G. Parr, Phys. Rev. B **37**, 785 (1988).

[54] A. D. Becke, J. Chem. Phys. **98**, 1372 (1993).

[55] J. Ireta, J. Neugebauer, and M. Scheffler, J. Phys. Chem. A **108**, 5692 (2004).

[56] E. J. Meijer and M. Sprik, J. Chem. Phys. **105**, 8684 (1996).

[57] S. M. Cybulski and C. E. Seversen, J. Chem. Phys. **122**, 014117 (2005).

[58] W. Klopper, J. G. C. M. van Duijneveldt-van de Rijdt, and F. B. van Duijneveldt, Phys. Chem. Chem. Phys. **2**, 2227 (2000).

[59] J. Olsen and P. Jørgensen, J. Chem. Phys. **82**, 3235 (1985).

[60] DALTON, a molecular electronic structure program, Release Dalton2011 (2011), see `http://daltonprogram.org/`.

[61] P. Jørgensen, H. J. Aa. Jensen, and J. Olsen, J. Chem. Phys. **89**, 3654 (1988).

[62] P. Sałek, O. Vahtras, T. Helgaker, and H. Ågren, J. Chem. Phys. **117**, 9630 (2002).

[63] C. Hättig, O. Christiansen, H. Koch, and P. Jørgensen, Chem. Phys. Lett. **269**, 428 (1997).

[64] M. H. Levitt, *Spin Dynamics: Basics of Nuclear Magnetic Resonance* (Wiley, Chichester, 2001).

[65] A. Florin and M. Alei, Jr., J. Chem. Phys. **47**, 4268 (1967).

[66] W. T. Raynes, Mol. Phys. **49**, 443 (1983).

[67] J. C. Hindman, J. Chem. Phys. **44**, 4582 (1966).

[68] W. T. Raynes, in *Nuclear Magnetic Resonance, A Specialist Periodical Report, Vol. 7,* p. 1 (Royal Society of Chemistry: London, 1978).

[69] K. Modig and B. Halle, J. Am. Chem. Soc. **124**, 12031 (2002).

[70] K. Wolinski, J. F. Hinton, and P. Pulay, J. Am. Chem. Soc. **112**, 8251 (1990).

[71] T. Helgaker and P. Jørgensen, J. Chem. Phys. **95**, 2595 (1991).

[72] R. Ludwig, F. Weinhold, and T. C. Farrar, J. Chem. Phys. **103**, 6941 (1995).

[73] P. Atkins and R. Friedman, *Molecular Quantum Mechanics* (Oxford University Press, 5th ed., 2011).

[74] A. D. Buckingham and P. J. Stephens, Annu. Rev. Phys. Chem. **17**, 399 (1966).

[75] A. D. Buckingham, Phil. Trans. R. Soc. A **293**, 239 (1979).

[76] L. R. Ingersoll and D. H. Liebenberg, J. Opt. Soc. Am. **48**, 339 (1958).

[77] C. E. Waring and R. L. Custer, J. Am. Chem. Soc. **74**, 2506 (1952).

[78] A. Balbin Villaverde and D. A. Donatti, J. Chem. Phys. **71**, 4021 (1979).

[79] T-t. Lu, M. He, D-m. Chen, T-j. He, and F-c. Liu, Chem. Phys. Lett. **479**, 14 (2009).

[80] T. Helgaker, M. Jaszuński, and K. Ruud, Chem. Rev. **99**, 293 (1999).

[81] J. Vaara, Phys. Chem. Chem. Phys. **9**, 5399 (2007).

[82] J. Tomasi, B. Mennucci, and R. Cammi, Chem. Rev. **105**, 2999 (2005).

[83] K. V. Mikkelsen, P. Jørgensen, K. Ruud, and T. Helgaker, J. Chem. Phys. **106**, 1170 (1997).

[84] M. Cossi and O. Crescenzi, J. Chem. Phys. **118**, 8863 (2003).

[85] K. V. Mikkelsen, K. Ruud, and T. Helgaker, Chem. Phys. Lett. **253**, 443 (1996).

[86] D. B. Chesnut and B. E. Rusiloski, J. Mol. Struct. (THEOCHEM) **314**, 19 (1994).

[87] D. Sebastiani and M. Parrinello, J. Phys. Chem. A **105**, 1951 (2001).

[88] F. Mauri, B. G. Pfrommer, and S. G. Louie, Phys. Rev. Lett. **77**, 5300 (1996).

[89] V. G. Malkin, O. L. Malkina, G. Steinebrunner, and H. Huber, Chem. Eur. J. **2**, 452 (1996).

[90] B. G. Pfrommer, F. Mauri, and S. G. Louie, J. Am. Chem. Soc. **122**, 123 (2000).

[91] R. E. Wasylishen and D. L. Bryce, J. Chem. Phys. **117**, 10061 (2002).

[92] G. Cazzoli, L. Dore, C. Puzzarini, and S. Beninati, Phys. Chem. Chem. Phys. **4**, 3575 (2002).

[93] J. Vaara, J. Lounila, K. Ruud, and T. Helgaker, J. Chem. Phys. **109**, 8388 (1998).

[94] S. Kirkpatrick, C. D. Gelatt, Jr., and M. P. Vecchi, Science **220**, 671 (1983).

[95] J. VandeVondele, F. Mohamed, M. Krack, J. Hutter, M. Sprik, and M. Parrinello, J. Chem. Phys. **122**, 014515 (2005).

[96] S. Izvekov and G. A. Voth, J. Chem. Phys. **116**, 10372 (2002).

[97] I.-F. W. Kuo, C. J. Mundy, M. J. McGrath, J. I. Siepmann, J. VandeVondele, M. Sprik, J. Hutter, B. Chen, M. L. Klein, F. Mohamed, et al., J. Phys. Chem. B **108**, 12990 (2004).

[98] I.-F. W. Kuo and C. J. Mundy, Science **303**, 658 (2004).

[99] The FINGER program has mainly been developed in the Helsinki University of Technology, Espoo, Finland. It is based on techniques presented in the paper by K. Laasonen, A. Pasquarello, R. Car, C. Lee, and D. Vanderbilt, Phys. Rev. B **47**, 10142 (1993).

[100] B. Guillot, J. Mol. Liq. **101**, 219 (2002).

[101] R. Ludwig, Angew. Chem. Int. Ed. **40**, 1808 (2001).

[102] F. N. Keutsch and R. J. Saykally, Proc. Natl. Acad. Sci. **98**, 10533 (2001).

[103] J. L. Finney, Phil. Trans. R. Soc. Lond. B **359**, 1145 (2004).

[104] R. Kumar, J. R. Schmidt, and J. L. Skinner, J. Chem. Phys. **126**, 204107 (2007).

[105] M. Matsumoto and I. Ohmine, J. Chem. Phys. **104**, 2705 (1996).

[106] M. Mezei and D. L. Beveridge, J. Chem. Phys. **74**, 622 (1981).

[107] A. Luzar and D. Chandler, Phys. Rev. Lett. **76**, 928 (1996).

[108] C. Eckart, Phys. Rev. **47**, 552 (1935).

[109] H. Cybulski and J. Sadlej, Chem. Phys. **323**, 218 (2006).

[110] M. Pecul and J. Sadlej, Chem. Phys. Lett. **308**, 486 (1999).

[111] M. Pecul, J. Lewandowski, and J. Sadlej, Chem. Phys. Lett. **333**, 139 (2001).

[112] R. Janoschek, Mol. Phys. **89**, 1301 (1996).

[113] J. Kongsted, K. Aidas, K. V. Mikkelsen, and S. P. A. Sauer, J. Chem. Theory Comput. **4**, 267 (2008).

[114] M. G. Müller, B. Kirchner, P. S. Vogt, H. Huber, and D. J. Searles, Chem. Phys. Lett. **346**, 160 (2001).